

Locating the Seattle Fault in Bellevue, WA: Combining geomorphic indicators with borehole data

Rebekah Cesmat

**A report prepared in partial fulfillment of
the requirements for the degree of**

**Master of Science
Earth and Space Sciences: Applied Geosciences**

University of Washington

November 2014

Project mentor:

Brian Sherrod, U.S. Geological Survey, Research Geologist; University of Washington affiliate faculty

Internship coordinator:

Kathy Troost

Reading committee:

Alison Duvall

Kathy Troost

Juliet Crider

MESSAGe Technical Report Number: [014]

©Copyright 2014

Rebekah Cesmat

Abstract

The Seattle Fault is an active east-west trending reverse fault zone that intersects both Seattle and Bellevue, two highly populated cities in Washington. Rupture along strands of the fault poses a serious threat to infrastructure and thousands of people in the region. Precise locations of fault strands are still poorly constrained in Bellevue due to blind thrusting, urban development, and/or erosion. Seismic reflection and aeromagnetic surveys have shed light on structural geometries of the fault zone in bedrock. However, the fault displaces both bedrock and unconsolidated Quaternary deposits, and seismic data are poor indicators of the locations of fault strands within the unconsolidated strata. Fortunately, evidence of past fault strand ruptures may also be recorded indirectly by fluvial processes and should also be observable in the subsurface. I analyzed hillslope and river geomorphology using LiDAR data and ArcGIS to locate surface fault traces and then compare/correlate these findings to subsurface offsets identified using borehole data. Geotechnical borings were used to locate one fault offset and provide input to a cross section of the fault constructed using Rockworks software. Knickpoints, which may correlate to fault rupture, were found upstream of this newly identified fault offset as well as upstream of a previously known fault segment.

Table of Contents

1 Introduction	1
2 Scope of Work	2
3 Background	3
3.1 <i>Tectonic setting</i>	3
3.2 <i>Quaternary stratigraphy and lithology</i>	4
3.3 <i>Extracting tectonic information from stream channels</i>	5
4 Methods	6
4.1 <i>Data acquisition</i>	7
4.2 <i>Digital geomorphic analysis</i>	7
4.3 <i>Borehole analysis</i>	8
4.4 <i>Field Investigation</i>	9
5 Assumptions and Limitations	9
5.1 <i>Urbanization</i>	10
5.2 <i>Caveats in calculating slope-area data</i>	10
5.3 <i>Errors contained in geotechnical borings</i>	11
5.4 <i>GPR challenges</i>	11
6 Results	12
6.1 <i>Digital geomorphic analysis</i>	12
6.2 <i>Borehole analysis</i>	12
6.3 <i>Ground penetrating radar</i>	13
7 Discussion	13
7.1 <i>Surface analysis</i>	13
7.2 <i>Subsurface analysis</i>	14
7.3 <i>Hazard summary</i>	15
8 Conclusions	15
9 References cited	17
10 Figures	20
Figure 1.....	20
Figure 2.....	21
Figure 3.....	22
Figure 4.....	23
Figure 5.....	24
Figure 6.....	25

Figure 7.....	25
Figure 8.....	26
Figure 9.....	27
Figure 10	28
Figure 11	28
Figure 12	28
Figure 13	29
Figure 14	30
Figure 15	31
Figure 16	32
Figure 10	33
Figure 18	34
Figure 19	35
Figure 20	36
Figure 21	37
Figure 22	38
Figure 23	39
Figure 24	40
Figure 25	41
Figure 26	42
Figure 27	43
Table 1.....	44
Figure 28	45
Figure 29	46
Figure 30	47
Figure 31	48
Figure 32	49
Figure 33	50

Acknowledgements

This project would not have come together without the help from many people. I'd like to thank Kathy Troost for her intellectual contribution; Brian Sherrod for making the time to be the project mentor; Matt Benson with Golder Associates for loaning us GPR equipment; Sue Bednarz from Jacobs Associates for her insight, data, and allowing us to observe drilling; Bryan Holmes for his collaboration; Juliet Crider for her assistance with my GSA presentation and report reviews; and Alison Duvall for her review contribution. I'd also like to make a special acknowledgement to the GSA Park D. Snavely Cascadia Research Award and the ExxonMobil sponsored graduate student research award.

1 Introduction

Active crustal thrust faults can be difficult to study when surficial traces are either removed, masked, or never formed. These challenges are amplified in locations such as western Washington where an erosive climate, urbanization and blind thrusting affect surficial fault expression. The Seattle Fault is an active thrust fault zone with a poorly constrained location through Bellevue, WA. My goal in this study is to determine the surficial location of major fault strands of the Seattle Fault Zone (SFZ) in Bellevue by characterizing the extent of deformation both at the surface and in the subsurface. I use existing borehole and seismic reflection data combined with an analysis of hillslope and stream channel morphology to improve our knowledge of the spatial location of strands of the fault. This study outlines a method for characterizing blind thrust faults using a broad spectrum of data analysis techniques.

The nature of the geologic setting creates a challenging environment for fault investigations. In the Puget Lowland, bedrock has limited exposure because it is blanketed by Quaternary glacial and interglacial deposits. In a few locations, uplift as a result of crustal faulting has exhumed Tertiary bedrock. Direct observations of bedrock provide the most robust level of detail, so fault investigations are, in most cases, limited to indirect detection methods of buried bedrock. Geophysical techniques are one of the primary methods of investigating Puget Lowland crustal faults (Blakely *et al.*, 2002, Brocher *et al.*, 2004, Clement *et al.*, 2010, Johnson *et al.*, 1996, Liberty and Pratt, 2008, ten Brink *et al.*, 2002). In undeveloped locations where the fault has ruptured since deglaciation, surface fault traces can often be identified using bare earth LiDAR. Because this is an active fault zone that intersects two cities populated with approximately 750,000 people, continuing to study the fault is important and it aids in defining hazards associated with shaking and rupture.

This study focuses on the eastern extent of the SFZ in eastern Bellevue, WA (Figure 1). The results of this study benefit the greater Bellevue community by enhancing published geologic maps (Troost and Wisner, 2012) and illustrating the need to define hazard zones associated with fault rupture. Fault offset, ground rupture, and shaking of unconsolidated material poses a significant threat to people and infrastructure, including secondary hazards such as landsliding, tsunamis, and flooding. Improving the known location of the SFZ aids in better defining and preparing for those hazards.

In order to improve fault strand locations, I focus on two investigative approaches in this study: 1) surface analysis and 2) subsurface analysis. Correlating subsurface data with an analysis of surficial processes associated with fault uplift will help to further define the characteristics of the SFZ.

Surface analysis: This portion of the study uses digital elevation data to characterize stream channel and topographic morphology in order to assess past fault rupture from the surface response. The morphology of stream channels and hillslopes are known to be influenced by tectonics (e.g. Kirby and Whipple, 2012) and thus may reveal recent fault zone activity.

Subsurface analysis: The second portion of this study utilizes an extensive borehole dataset to locate lithologic offsets in the subsurface. In the eastern Bellevue, geotechnical borings have not yet been used as an aid in search for lithologic offsets indicative of faulting. I determine the viability of this technique in Quaternary stratigraphy and in bedrock. Rockworks software is used to create images of the stratigraphy found in borehole logs plotted on topographic surface profiles. These graphics allow visualization of stratigraphic offsets along the study section. I project these offsets to the surface and use GPR surveys to validate these findings.

2 Scope of Work

This project focuses on producing maps and figures that illustrate findings related to fault deformation at the surface and subsurface. I use three distinct yet complementary analyses to study the SFZ: surficial analyses of river channels and topography, subsurface analyses of underlying units, and field observations which includes familiarization of geologic units and GPR surveys. This study remains within eastern Bellevue, from just north of Interstate 90 to the southern extent of Lake Sammamish. This study area includes the northern extent of the SFZ, which incorporates a more recently active strand in eastern Bellevue (Sherrod, 2002). Rupture on the Vasa Park strand occurred between 16,000 and 4500 years BP (Sherrod, 2002).

3 Background

3.1 Tectonic setting

Active crustal faults in the Puget Lowland result from crustal shortening along the western margin of the North American plate, on the hanging wall of the Cascadia Subduction Zone (Figure 2). The western margin of the North American plate is subdivided into the Sierra Nevada, Oregon, and Washington blocks that are compartmentalized by differing Neogene deformation styles. (Wells *et al.*, 1998). The Sierra Nevada block is migrating to the northwest, which causes the Oregon block to accommodate movement with clockwise rotation. The Washington block absorbs this rotation with transpressional deformation, creating thrust and reverse crustal faults (Figure 2). Geodetic data from the North American Plate reveals that the motion of these crustal blocks is oblique to, and in some locations, parallel to the Cascadia Subduction zone (McCaffery *et al.*, 2007; Figure 3).

Crustal faults in the Puget Lowland have an east-west and northeast-southwest strike with a northward vergence (Johnson *et al.*, 1999; Figure 2). These faults create a series of uplifts and basins (Figure 4). Glacial and interglacial stratigraphy fills the basins and the uplifted regions comprise Tertiary bedrock units (Figures 4, 9). The east-west trending faults are thrust or reverse faults that have mostly vertical motion and are oriented sub-perpendicular to the Cascadia Subduction Zone (Johnson *et al.*, 1998). The northwest-southeast trending faults are also thrust or reverse faults that have components of vertical and transform motion; these faults accommodate transpressional deformation that is oblique to the subduction zone (Johnson *et al.*, 1998). Approximately 4-7 mm/yr of crustal shortening is accommodated by these faults as determined using GPS and velocity data (Mazzotti *et al.*, 2002). In the Puget Sound region, upper plate motion has an average shortening rate of 4.4 ± 0.3 mm/yr (McCaffery *et al.*, 2007).

The SFZ extends from the Olympic Peninsula to the Cascade volcanic province (Figures 1, 4). To date, researchers have proposed many competing fault geometries based on geophysical techniques including gravity, aeromagnetic, and seismic surveys (ten Brink *et al.*, 2002, Brocher *et al.* 2004, Kelsey *et al.*, 2008, Liberty and Pratt, 2008, Nelson *et al.*, 2014; Figure 5). One commonality shared by all of these models is the change in depth to bedrock on either side of the fault. To the north of the SFZ lies the Seattle Basin, and to the south lies the Seattle Uplift; maximum bedrock offset was observed between these two features (Blakely *et al.*, 2001).

Approximately 8 km of Quaternary glacial and interglacial deposits fill the Seattle Basin (Liberty and Pratt, 2008). The Seattle Uplift exposes bedrock at the surface as a result of crustal shortening and uplift along the SFZ. The eastern extent of the SFZ has been modeled with one main antiformal back thrust that connects to the master ramp at depth (Liberty and Pratt, 2008; Figure 6). Other fault models of the western and central fault zone are modeled with back thrusts that connect to the master ramp at depth, but do not contain folding (ten Brink *et al.*, 2002, Kelsey *et al.*, 2008, Nelson *et al.*, 2003; Figure 5). Some fault models contain strands that are blind thrusts (Kelsey *et al.*, 2008). Although, geophysical techniques have proven useful in identifying fault strands at a gross scale, the finer details of fault strand locations are not easily defined by these techniques.

Trenching across the fault zone has also been a useful tool in investigating fault structure and rupture history. Analyzing the extensive Puget Sound LiDAR Consortium (PSLC) LiDAR datasets is a common tool in Puget Lowland fault investigations. The Toe Jam Hill fault scarp, located on Bainbridge Island, is the first fault scarp in the Puget Lowland that was detected using LiDAR (Nelson *et al.*, 2003). Trenching across this fault revealed that rupture of approximately 36 km along the fault occurred along north-dipping back thrusts that are antithetic to the master thrust (Nelson *et al.*, 2003; Figure 7). Additional trenching across the SFZ in Vasa Park in Bellevue, WA revealed the eastern extent of fault deformation at the surface where bedrock is thrust over glacial units (Sherrod, 2002). Carbon dates bracket this event to between 16,000 and 4,500 years ago (Sherrod, 2002).

Geophysical investigations have yielded approximate slip rates on the fault through indirect observations of bedrock and along fault scarps, short-term slip rates were determined. Paleoseismic studies, such as at the Toe Jam Hill fault scarp, in the western extent of the SFZ, document an approximate slip rate of 0.2 mm/yr for the past 16,000 years and a slip rate of 2 mm/yr for the past 2500 years (Nelson *et al.*, 2003). Seismic-reflection profiles yielded a similar slip rate of 0.7- 1.1 in the western extent of the SFZ from Lake Washington to Hood Canal (Johnson *et al.*, 1999) and 0.25 mm/yr for the eastern extent in Bellevue (Liberty and Pratt, 2008).

Liberty and Pratt (2008) and Sherrod (2002) concluded that the scarp-forming deformation front is located at the offset identified in the USGS paleoseismology trench at Vasa Park. To the south of the deformation front, backthrusts with north-side-up motion are

identifiable in seismic surveys. These backthrusts connect to a master ramp thrust at a depth of approximately 8 km, but this depth is not confirmed because the resolution of seismic data can be lost at this depth (Liberty and Pratt 2008). A hinge surface of the monoclinical deformation projects to the north side of I-90 (Figure 8). The eastern extent of the SFZ is interpreted to have a fault-bend-fold geometry (Liberty and Pratt, 2008).

3.2 Quaternary stratigraphy and lithology

The Puget Lowland has an extensive glacial history where many glacial cycles have shaped and reshaped the modern landscape. Glaciers have carved uplifted bedrock, deposited un lithified sediments, retreated, and then returned to consolidate older sediments and deposit new glacial sediments. Interglacial deposits accumulated between glacial advance and after the most recent retreat. Quaternary deposits are laterally discontinuous and are of varying thicknesses. Quaternary units can overlie bedrock as a stratigraphic contact, or as a fault contact in locations where fault offset juxtaposes bedrock against glacial units, such as in the Vasa Park trench mentioned above.

Tertiary bedrock units compose the Seattle Uplift (Figure 9). These are marine and terrestrial sedimentary rocks that are highly weathered near the surface and are sometimes poorly lithified. In the study area, three bedrock formations can be found: Upper Eocene Renton Formation, Upper Eocene and Oligocene Blakeley Formation, and Lower Miocene Blakely Harbor Formation.

- The Upper Eocene Renton Formation is a nonmarine sandstone with interbedded carbonaceous siltstone, coal, and claystone (Yount and Gower, 1991).
- The Upper Eocene and Oligocene Blakeley Formation is a marine siltstone and sandy siltstone with tuffaceous fine to coarse grained volcanic rich sandstone (Yount and Gower, 1991). This formation also contains pebble to cobble conglomerate units containing rounded to subrounded andesite and basalt clasts.
- The Lower Miocene Blakely Harbor Formation is a nonmarine thick bedded pebble to cobble conglomerate containing basaltic clasts with minor amounts of metamorphic rock, greywacke, chert, and felsic volcanic rock (Yount and Gower, 1991).

Since deglaciation approximately 15,000 years ago, rivers and streams have carved the glacial landscape. In the study area, the climate and the nature of the Quaternary sediments

create erodible terrains that are densely vegetated. The glacial and interglacial stratigraphy, landscape, vegetation, and urbanization create challenging conditions for studying crustal faults.

3.3 *Extracting tectonic information from stream channels*

Streams in eastern Bellevue deflect as they cross the fault zone, which is typically seen in strike-slip fault regimes. A geomorphic analysis of these streams, compared to an analysis of streams outside the fault zone aids in determining if this deflection is fault related (Figure 10). Fault rupture would create knickpoints in the channels, which are observable as abrupt disruptions in the equilibrium graded stream profile. Another mode of deformation that could disrupt stream incision is blind thrusting. Some strands of the SFZ are blind faults that do not intersect the surface, so these strands may create a differing signature in the stream channels.

In tectonically active regions, such as the Puget Lowland, tectonic uplift and erosion steepens landscapes and creates relief (Montgomery and Brandon, 2002). A record of tectonic uplift can be extracted from an analysis of longitudinal profiles of stream channels and their drainage basins (Whipple and Tucker, 1999). In most natural settings, stream channels exhibit a power-law relationship between drainage area and channel slope (e.g. Flint, 1974, Hack, 1973):

$$S = k_s A^{-\theta}$$

where S is local channel slope, A is drainage area, k_s and θ are the steepness and concavity indices (Wobus *et al.*, 2006). Digital topographic data can be used to extract slope and drainage area information for a given landscape. By plotting slope vs. upstream drainage area on a logarithmic scale, we can identify a linear relationship within the fluvial realm (Figure 10). Streams in equilibrium, where erosion rates are constant, and there are no disruptions to baselevel, will have a predictable graded profile that has a concave shape (Mackin, 1948; Figure 11). Along a longitudinal profile, knickpoints are identifiable as an abrupt decrease in elevation with respect to distance. These locations also correspond to abrupt changes in slope vs. drainage area plots. Knickpoints are caused by a change in baselevel of the drainage network or by a change in erosion rate of the bed material (Figure 12). These knickpoints disrupt equilibrium state within the stream channel. Changes in baselevel may be associated with coseismic uplift, changes in stream power, or changes in stream outlet elevation.

4 Methods

This project includes three discreet analyses that each provide a different perspective of the geological conditions in eastern Bellevue. First, I employed a digital geomorphic analysis that focusing on streams in the study area in order to characterize surface fault activity. Second, I analyzed the subsurface using existing boreholes in the GeoMapNW database (Troost, written communication). Using Rockworks software, I generated plots of subsurface lithologies from the raw boring log data. Finally, I conducted GPR surveys of specific field sites identified by the other two methods. A combination of these geomorphic and borehole analyses aids in determining the fault characteristics at both the surface and subsurface.

4.1 Data acquisition

I obtained LiDAR hillshades and DEM maps from the Puget Sound LiDAR Consortium. The LiDAR data has a 6-foot resolution. The Washington State Department of Natural Resource's fault and fold database is the primary data source for previously identified locations of major fault strands within the SFZ. This study focuses on locating smaller-scale strands not previously found. I use borehole data compiled by GeoMapNW from 1998-2012 as the primary data source in locating offsets in the subsurface (Troost and Booth, 2008). These data are currently hosted by the Washington State DNR website (<https://fortress.wa.gov/dnr/geology/?Theme=subsurf>).

The PSLC manages and distributes freely a compiled data set of all LiDAR in the Puget Sound region. These data were originally compiled as a comprehensive search for fault rupture (<http://pugetsoundlidar.ess.washington.edu>). I use 6-foot resolution LiDAR elevation datasets sourced from the PSLC in surface investigations of this study.

4.2 Digital geomorphic analysis

The first process in this fault investigation, utilizes visual observation of LiDAR hillshade maps. Using ArcGIS and a bare earth LiDAR hillshade, I illustrated linear features within the fault zone. This map aided in identifying locations of interest for geomorphic, borehole, and field investigations. I will refer to this map as the lineament map (Figure 14).

In order to analyze hillslope and stream morphology of southern Bellevue, I analyze LiDAR elevation data using the TecDEM landscape analysis code that runs in Matlab (Shahzad

and Gloaguen, 2010). I used TecDEM to create slope-area plots (Figure 10) for stream channels upstream of the fault within the study area. Stream profiles were analyzed for knickpoints potentially related to motion on the fault which crosses the analyzed streams (Figure 10). First, the DEM needed to be “Filled” by removing holes in the data that are an artifact of DEM creation. Next, watersheds were delineated, and flow directions were determined. After these DEM preparation steps, I created a drainage density plot overlaid onto a DEM (Figure 15) from which I extracted longitudinal profiles of stream channels. I analyzed individual longitudinal profiles, for knickpoints which were marked and saved in order to create final stream analysis graphs. Knickpoint locations were then displayed in map view for each stream and compared to one another by location with respect to the fault (Figure 10).

4.3 Borehole analysis

Importing GeoMapNW borehole data into Rockworks allows us to analyze subsurface geology and locate abrupt changes in stratigraphy between closely spaced boreholes. Investigating the subsurface began by filtering borehole data in ArcGIS. The complete GeoMapNW dataset contains more than 80,000 borings in the greater Seattle area (Troost and Booth, 2008). Most of these data are not useful to this investigation and so, require filtration. Many of these borings are between 0-10 feet deep, and so do not contain enough detail of the subsurface to be useful to this investigation. I removed all borings 10 feet deep or less and then symbolized the remaining points to scale with exploration depth. Overlaying these data points onto a LiDAR hillshade helped to visualize where deep borings are found near lineaments (Figure 16).

An unmanageable number of borings remained after filtering for depth, so I focused investigations to areas of interest defined by the lineament map. Using the scale-to-depth map, I created a subset by looking for trends of north-south oriented clusters of borings. Of these selected borings, I looked at the detail of individual layers in the boring log data to determine which borings could provide the most information. These details included the presence of: bedrock and its depth, a Quaternary unit-bedrock contact and the nature of that contact, presence of highly fractured bedrock, interpreted Blakeley Formation, and presence of slickensides. This resulted in a subset of 358 borings, which was the basis for the rest of my investigation.

Next, I imported two datasets into Rockworks; these include topographic data and data from the selected borings. Topographic data acquired from the PSLC is displayed as a raster-type grid model of the LiDAR digital elevation data exported from ArcGIS. This grid model is necessary in creating topographic profiles to display along with the borehole striplogs. A borehole striplog is a visual representation of subsurface lithologies. Borehole data include, location, boring elevation and depth, layer thickness, and lithologic unit. I used these data to plot boring strip logs on a topographic profile. These plots are meant to illuminate offsets within the subsurface. I created boring striplogs across lineaments that I identified using the LiDAR analysis (Figure 14).

In Rockworks, striplog data can be displayed either as a point-to-point boring selection or as a swath profile selection. The point-to-point selection method allows borings to be individually selected and displayed along a topographic profile. Ideally, this method would be used by selecting points in a mostly straight, north-south oriented line. However, borings of interest are not all placed this way. I assume that a north-south line will be perpendicular to the strike of the fault and therefore will illustrate offsets most accurately. Point-to-point profile lines that are not oriented north-south may show apparent offsets rather than true offsets. The swath profile method projects boring logs onto an interpolated two dimensional topographic line that has the potential to show true offsets in the bedrock. However, resulting figures in Rockworks display data that is clustered and unmanageable to interpret. In these cases, some lower quality/shallower borings were removed so that the visuals aided the interpretations (Figure 17). I used both methods to create cross sections perpendicular to the strike of the fault and to display the subsurface lithology. Investigations were focused near lineaments identified in the LiDAR and at the borings of interest. Final strip-log profiles were created using Adobe Illustrator. These figures display the topographic profile, thickness, depth, and lithology.

I test and validate findings from the borehole analysis by comparing my results to results of previous researchers. Liberty and Pratt's (2008) seismic line survey data in Bellevue, WA is the main source of comparison because of the close proximity to this study site.

4.4 Field Investigation

After identifying areas of interest in the geomorphic and borehole investigations, I used GPR to determine more precise locations of subsurface offsets. GPR is a geophysical tool used to

view the shallow subsurface using sound waves to penetrate the ground. The GPR equipment used in this study had a 100 MHz antenna. Lower frequency antennas, such as the one used in this study, are used to reach a maximum penetration depth with lower subsurface resolution. Higher frequency antennas will provide higher resolution at a shallower depth (Matt Benson, personal communication). GPR surveys were limited to streets or trails that have a mostly north-south orientation because of housing developments and dense vegetation. Therefore, some of the GPR surveys were moved to more functional areas. Whether along streets or trails, unfavorable subsurface conditions affected the outcome of our results.

5 Assumptions and limitations

In order to produce meaningful results from this study, some assumptions about the geology must be made:

- The stratigraphy in the subsurface is laterally continuous on the scale of the topographic profiles created in Rockworks.
- Fault offsets appear in borehole sections as vertical or near vertical changes in the stratigraphy between two closely spaced boreholes.
- Boring logs are a reliable source of the subsurface stratigraphy.
- Bedrock and Quaternary deposits have differing erosion rates.

These assumptions are useful to the analyses presented in this study. However, each of these contains specific caveats described below.

5.1 Urbanization

Urbanization within the study area will affect the outcome of my results by increasing surface runoff into channels which therefore increases stream power. In order to minimize the effects, I focus my study to stream channels where less development has taken place.

Urbanization is typically confined to hilltops, and so I will focus this study on slopes that I assume to be less altered by construction or development. However, these slopes direct surface runoff into stream channels which may be increased as a result of urbanization, so the findings from this study will likely be skewed. Increased stream power also increases the rate at which

knickpoints propagate through the stream channels. The effects of urbanization include, creation of a knickpoint, or increasing knickpoint propagation rate.

5.2 Caveats in calculating slope-area data

Using the formula, $S = k_s A^{-\theta}$ as a basis for creating slope-area graphs and longitudinal profiles to find knickpoints contains inherent errors. This relationship does not account for changes in incision rate of the bed as a result of variability in the geologic conditions, or drainage area and slope caused by mass wasting events (Wobus *et al.*, 2006). Climactic effects on incision rates are also not considered in this formula (Wobus *et al.*, 2006). However, because geomorphology studies are conducted within a small area, I assume that there are no significant changes in climate, and there were no significantly large mass wasting events to have affected the channels. Changes in bed material is considered when analyzing the spatial location of knickpoints.

5.3 Errors in using geotechnical borings

Geotechnical borings, in some cases, do not contain enough lithologic information to interpret fault locations. For example, bedding is not typically recorded when it could provide crucial information in fault investigations. Bedding orientations could be used to project surfaces to detect offsets, or interpret structures. The nature of stratigraphic contacts may be lost during drilling. Fluid flow along fault zones can create zones of oxidation or decreased grain size that is valuable in indicating faulting; this essential information may not be properly recorded or it may be difficult to observe during drilling. In some cases, bedrock units are difficult to distinguish from glacial or interglacial deposits. Misinterpreted strata in borings are not a reliable data source and in these cases, reinterpretation of the boring logs may be necessary.

Utilizing borehole data to locate faults is not always reliable. Borings are not typically logged with a scientific perspective. Rather, they are drilled with the engineering or environmental properties of earth materials in mind, so many important details about the geology can be lost. In few cases where borings reach bedrock, where they provide an adequate amount of detail, and where they are densely spaced, it is possible to locate offsets using this method. Given the nature of the glacial history in this region, paleotopographic features could create

apparent, not real, offsets, and so, findings from borings may not always be accurate. It is necessary to test these findings using other fault investigation methods.

Identifying offsets in the subsurface is more effective in bedrock than in glacial units. Because glacial stratigraphy is laterally discontinuous, and boring logs are not always reliable, bedrock is the most robust indicator of subsurface offsets. However, in this region, boring excavations typically terminate once bedrock is encountered, or they do not encounter bedrock at all. This limits the availability of bedrock data which therefore limits the potential of using borehole data to identify faults. Quaternary deposits have lateral variability in grain size, sorting, and compaction, and they are not laterally continuous in the study area. As a result, locating offsets in Quaternary deposits is unlikely.

5.4 GPR challenges

Ground and subsurface conditions in the study area create challenges for field investigations using Ground Penetrating Radar (GPR). Utilities, high water table, and clayey soils skew the GPR data by creating highly reflective surfaces that block the view of the deeper subsurface. An ideal survey site would have unconsolidated, dry sandy soils overlying shallow bedrock.

6 Results

6.1 Digital Geomorphic analysis

Visual observation of bare earth LiDAR can provide insight into the landscape history and development. Uplift along the hanging wall of the Seattle Fault in the study area affects the planview shape of stream channels. Slope faces that divert stream flow across the hanging wall trend east-west, which is parallel to the mapped trend of the fault. These slope faces may indicate the location of one active strand of the fault. Lineaments in the study area trend mostly east-west, and some trend northwest-southeast in higher elevations where bedrock is exposed (Figure 14). Lineaments are more closely spaced in the southern extent of the study area.

Longitudinal profiles and slope vs. upstream drainage area plots illustrate that many of the streams that flow across the fault have knickpoints (Figures 18, 19, 20, 21). These knickpoints correspond to transition zones in the slope/area data of varying widths. Streams S2,

S3, and S4 in the fault zone contain knickzones that are wider than the knickzone in Stream S1. Streams S2 and S4 converge toward the outlet, and so the knickpoints map in the same location along the stream channel. Streams S2, S3, and S4 have knickpoints that plot at approximately 400 ft elevation. Stream S1 has a knickpoint at approximately 600 ft elevation. To test if these knickpoints are caused by fault rupture or are caused by a different disruption in the drainage network, I analyze stream channels outside the fault zone as well (Figures 10, 22). These streams do not show prominent knickpoints (Figures 23, 24, 25).

6.2 Borehole analysis

An analysis of geotechnical borings illustrated as striplogs and plotted onto topographic profiles aided in interpreting the subsurface. One bedrock offset was identified in the southeast corner of the study area with north-side-up motion (Figures 27). Bedrock is offset by approximately 30 ft. Boring logs in this area have strong evidence for faulting (Table 1, Figure 28) including notations on brecciated tuff, slickensides, and intense fracturing with mineralization along those fractures. This offset was identified along the cross section line A to A' (Figure 26, 27). To the west of this feature, along strike of the fault, bedrock is shallower to the north of the fault; this is observable in boreholes and on the geological map (Figure 29).

6.3 Ground Penetrating Radar

GPR profiles were unsuccessful in locating subsurface offsets due to the nature of the ground conditions. Along one transect in western Bellevue, I was able to identify glacial features in the subsurface (Figure 31). These features most closely resemble push moraines found at the leading end of a glacier (van Overmeeren, 1998). In most of our surveys, bedrock was not close enough to the surface, the groundwater table was too high, utilities blocked the view, or the ground surface was too reflective to identify subsurface units. Many of these surveys were conducted on pavement, overlying some amount of road fill, which creates a highly reflective surface that blocks radar penetration.

7 Discussion

7.1 Surface analysis

Knickpoints in the study area stream channels can form for a variety of reasons including: changes in lake level (local baselevel), changes in stream erosive power due to urbanization, changes in lithology as the stream crosses from bedrock into unconsolidated glacial deposits, or fault rupture. Differing erosion rates between bedrock and Quaternary sediments would create a knickpoint in the stream channel. An increase in stream power resulting from increased runoff from urbanization could cause a knickpoint to propagate through the drainage basin. The knickpoint identified in TecDEM in stream S3 is likely lithologically controlled as it lies on the contact between Quaternary sediments and Tertiary bedrock (Figure 29). The knickpoint in stream S2 likely relates to something else as it lies within a singular glacial unit. In addition, the knickpoint lies upstream of the USGS paleoseismology trench at Vasa Park where fault rupture was identified, indicating that this knickpoint could be related to the same fault rupture. However, field investigation is necessary to confirm the reason for this slope change along the stream's longitudinal profile.

Streams in an area north of the fault do not show the same disruptions in longitudinal profile and in slope/area data as do streams that flow through the fault zone. This eliminates the possibility that the knickpoints could have been caused by a change in lake level as all analyzed streams flow into the same body of water and so should experience the same base level history. Absence of knickpoints in the northern streams does not necessarily rule out the possibility that the knickpoints were created by an increase in stream power due to urbanization because this would have a localized effect. The study sites may be exposed to differing amounts of runoff due to urbanization which would cause differing erosive power. Knickpoints through the fault zone are more likely caused by fault rupture or changes in lithology.

Streams within the study area that change direction as they flow through the fault zone have average convex longitudinal profiles, indicating that they are not in equilibrium. These streams have been carved since the last deglaciation approximately 15,000 years ago. These streams may be deflecting in this way because uplifted terrain is creating east-west trending slope faces that the streams flow around. Blind faulting may be creating the steeper uplifted terrain. Liberty and Pratt (2008) interpret a south-dipping thrust fault at the location of the east-west trending slope faces where the streams change direction (Figure 33). Glacial drumlins may also have an effect on the shape of stream channels because these streams are incising into the drumlins.

Lineaments that are more closely spaced in the southern extent of the fault zone may be a result of more well exposed faulting where deformation has occurred for a longer period of time. Because the SFZ is propagating northward, deformation is relatively younger at the north end of the fault zone (Johnson *et al.*, 1999, Kelsey *et al.*, 2008). These lineaments could also be related to bedding planes within the bedrock units and because the bedrock is better exposed in the southern extent of the fault zone, more lineaments are identifiable in the LiDAR.

7.2 Subsurface analysis

The offset identified along cross section A to A' has a north-side-up motion which is antithetic to the predicted dip of the master ramp thrust. The SFZ has a northward vergence with a master thrust that dips to the south (Johnson *et al.*, 1999; Figure 5). Thus, the offset identified along cross section A to A' may relate to a back thrust with a northward dip. Past studies (Liberty and Pratt, 2008) interpret similar back thrusts to be shallow faults that intersect the main thrust at some depth. The depth to which these faults intersect is problematic and still poorly understood because the resolution of the seismic data decreases with depth. These seismic lines were conducted west of the offset identified in this study and along strike of the mapped fault. I compare my findings to Liberty and Pratt's (2008) seismic line data and determine that my findings are consistent with their back thrust interpretation (Figure 30). I mapped a hypothesized fault along the length of uplifted bedrock observable in boreholes (Figures 26, 28, 29).

After locating this offset, I went back to the geomorphic investigation to determine if a knickpoint lies in the stream channel that crosses it (Figures 21, 28, 29). One knickpoint lies upstream of the offset which is consistent with a knickpoint that is related to fault rupture because knickpoints propagate upstream from their source (Whipple and Tucker, 1999). The knickpoint lies in bedrock, which could suggest a change in lithology within the bedrock unit, or it could suggest that the hypothesized fault ruptured and created a knickpoint that is propagating upstream.

7.3 Hazard summary

Findings from this study help to underscore the need to continue studying the SFZ as it is a direct hazard to large populations, yet the body of knowledge on the fault zone is not complete enough to define those hazards. Continuing to obtain a higher level of detail on the spatial

location of fault strands helps to define the zone over which fault rupture is likely to occur. As the state of knowledge continues to grow, it is important to inform the public of the risk associated with living or working within the hazard zone.

8 Conclusions

Geomorphic analysis of the fault zone show that stream channels contain knickpoints that are either related to fault rupture, a change in lithology, or an increase in erosive power due to urbanization. Streams in an area north of the SFZ do not contain knickpoints suggesting that there have been no significant disruptions to equilibrium incision rates. All knickpoints are located at different lengths along the stream channel suggesting that they were not caused by a change in lake level.

Borehole analysis revealed one bedrock offset between closely spaced boreholes that contain strong evidence for faulting including, breccia, slickensides, and oxidized surfaces. The offset has north-side-up motion which is consistent with findings from previous fault investigations. GPR surveys were inconclusive at refining fault locations due to the nature of the ground conditions. Of the methods presented in this study, the combination of previously acquired deep geophysical data and borehole data is the most robust way to locate unknown strands of the fault.

9 References cited

- Blakely, R. J., Wells, R. E., Weaver, C. S., and Johnson, S. Y. 2002. Location, structure, and seismicity of the Seattle Fault Zone Washington: Evidence from aeromagnetic anomalies, geologic mapping, and seismic reflection data. *Geological Society of America Bulletin*, vol. 114, no. 2, p. 169-177.
- Brocher, T. M., Blakely, R. J., and Wells, R. E., 2004. Interpretation of the Seattle Uplift, Washington, as a Passive-Roof Duplex. *Seismological Society of America*. vol. 94, no. 4, p. 1379-1401.
- Bull, W. B., 1979. Threshold of critical power in streams. *Geological Society of America Bulletin*, vol. 90, no. 5, p. 453-464.
- Clement, C., R. Pratt, Thomas L., Holmes, Mark L., and Sherrod, B. L., 2010. High-Resolution Seismic Reflection Imaging of Growth Folding and Shallow Faults beneath the Southern Puget Lowland, Washington State. *Bulletin of the Seismological Society of America*, vol. 100, no. 4, p. 1710-1723.
- Duvall, A., Kirby, E., and Burbank, D., 2004. Tectonic and lithologic controls on bedrock channel profiles and processes in coastal California. *Journal of Geophysical Research*, vol. 109, F03002.
- Flint, J. J., 1974. Stream gradient as a function of order, magnitude, and discharge. *Water Resources Research*, vol. 10, no. 5, p. 969-973.
- Hurst, M. D., Mudd, S. M., Attal, M., and Hilley, G., 2013. Hillslopes Record the Growth and Decay of Landscapes. *Science*, vol. 341, p. 868-871.
- Johnson, S. Y., Potter, C. J., Miller, J. J., Armentrout, J. M., Finn, C., and Weaver, C., 1996. The Southern Whidbey Island Fault: An active structure in the Puget Lowland, Washington. *Geological Society of America Bulletin*, vol. 108, no. 3, p. 334-354.
- Johnson, S. Y., Dadisman, S. V., Childs, J. R., and Stanley, W. D., 1999. Active tectonics of the Seattle fault and central Puget Sound, Washington – Implications for earthquake hazards. *Geological Society of America Bulletin*, vol. 111, no. 7, p. 1042-1053.
- Kelsey, H. M., Sherrod, B. L., Nelson, A. R., and Brocher, T. M., 2008. Earthquakes generated from bedding plane-parallel reverse faults above an active wedge thrust, Seattle fault zone. *Geological Society of America Bulletin*, vol. 120, no., 11 p. 1518-1597.
- Kirby, E., and Whipple, K. X., 2012. Expression of active tectonics in erosional landscapes. *Journal of Structural Geology*, vol. 44, p. 54-75.

- Liberty, L., and Pratt, T., 2008. Structure of the Eastern Seattle Fault Zone, Washington State: New Insights from Seismic Reflection Data. *Bulletin of the Seismological Society of America*, vol. 98, no. 4, p.1681-1695.
- Mackin, J. H., 1948. Concept of the graded river. *Geological Society of America Bulletin*, vol. 59, no. 5, p. 463-512.
- Mazzotti, S., Dragert, H., Hyndman, R. D., Miller, M. M., and Henton, J. A., 2002. GPS deformation in a region of high crustal seismicity: N. Cascadia forearc. *Earth and Planetary Science Letters*, vol. 198, p. 41-48.
- McCaffery, R., Qamar, A., I., King, R. M., Wells, R. E., Khazaradze, G., Williams, C., A., Stevens, C. W., Vollick, J. J., and Zwick, P. C., 2007. Fault locking, block rotation and crustal deformation in the Pacific Northwest. *Geophysical Journal International*, vol. 169, p. 1315-1340.
- Montgomery, D. R., and Brandon, M. T., 2002. Topographic controls on erosion rates in tectonically active mountain ranges. *Earth and Planetary Science Letters*, vol. 201, p. 481-489.
- Puget Sound LiDAR Consortium, 2014. *Data*. Retrieved from <http://pugetsoundlidar.ess.washington.edu>
- Nelson, A. R., Johnson, S. Y., Kelsey, H. M., Wells, R. E., Sherrod, B. L., Pezzopan, S. K., Bradley, L., Koehler III, R. D., and Buckman, R. C., 2003. Late Holocene Earthquakes on the Toe Jam Hill fault, Seattle fault zone, Bainbridge Island, Washington. *Geological Society of America Bulletin*, vol. 115, no. 11, p. 1388-1403.
- Nelson, A. R., Personius, S. F., Sherrod B. L., Kelsey, H. M., Johnson, S. Y., Bradley, L. A., Wells, R. E., 2014. Diverse rupture modes for surface-deforming upper plate earthquakes in southern Puget Lowland of Washington State. *Geosphere*, vol. 10., no. 4, p. 1-28.
- Shahzad, F., and Gloaguen, R., 2010. TecDEM: A MATLAB based toolbox for tectonic geomorphology, Part 1: Drainage network processing and stream profile analysis. *Computers & Geosciences*, vol. 37, p. 250-260.
- Sherrod, B. L., 2002. Fission track ages of Tertiary Bedrock in the hanging wall of the Seattle Fault Zone. *Geological Society of America, Cordilleran Section – 98th Annual Meeting*.
- Sherrod, B. L., 2002. Late Quaternary Surface Rupture along the Seattle Fault Zone Near Bellevue, Washington. *American Geophysical Union, Fall Meeting, 2002*, abstract #S21C-12.
- ten Brink, U.S., Molzer, P.C., Fisher, M. A., Blakely, R. J., Bucknam, R. C., Parsons, T., Crosson, R. S., and Creager, K. C., 2002. Subsurface Geometry and Evolution of the Seattle Fault Zone and the Seattle Basin, Washington. *Seismological Society of America*, vol. 92. no. 5, p. 1737-1753.

Troost K. G. and Booth, D. B., 2008. Geology of Seattle and the Seattle Area, Washington. *Geological Society of America, Reviews in Engineering Geology*, vol. XX, p. 1-35.

Troost, K. G. and Wisner, A. P., 2012. Geologic map of the City of Bellevue, WA, U. S. *Geological Survey Scientific Investigations Map*, scale 1:12,000.

van Overmeeren, R. A., 1998. Radar facies of unconsolidated sediments in The Netherlands: A radar stratigraphy interpretation for hydrogeology. *Journal of Applied Geophysics*, vol. 40 p. 1-18.

Washington State Department of Resources, 2014. Geological Information Portal.
<https://fortress.wa.gov/dnr/geology/?Theme=subsurf>

Wells, R. E., Weaver, C. S., and Blakely, R. J., 1998. Fore-arc migration in Cascadia and its neotectonic significance. *Geology*, vol. 26, no. 8, p. 759-762.

Whipple, K. X., and Tucker, G. E., 1999. Dynamics of the stream-power river incision model: Implications for height limits of mountain ranges, landscape response timescales, and research needs. *Journal of Geophysical Research*, v. 104, p. 661-674.

Wobus, C., Whipple, K. X., Kirby, E., Snyder, N., Johnson, J., Spyropolou, K., Crosby, B., and Sheehan, D., 2006. Tectonics from topography: Procedures, promise, and pitfalls. *Geological Society of America, Special Paper 398*.

Yount, J. C., and Gower, H. D., 1991. Bedrock geologic map of the Seattle 30' by 30' quadrangle, Washington. U.S. Geological Survey.

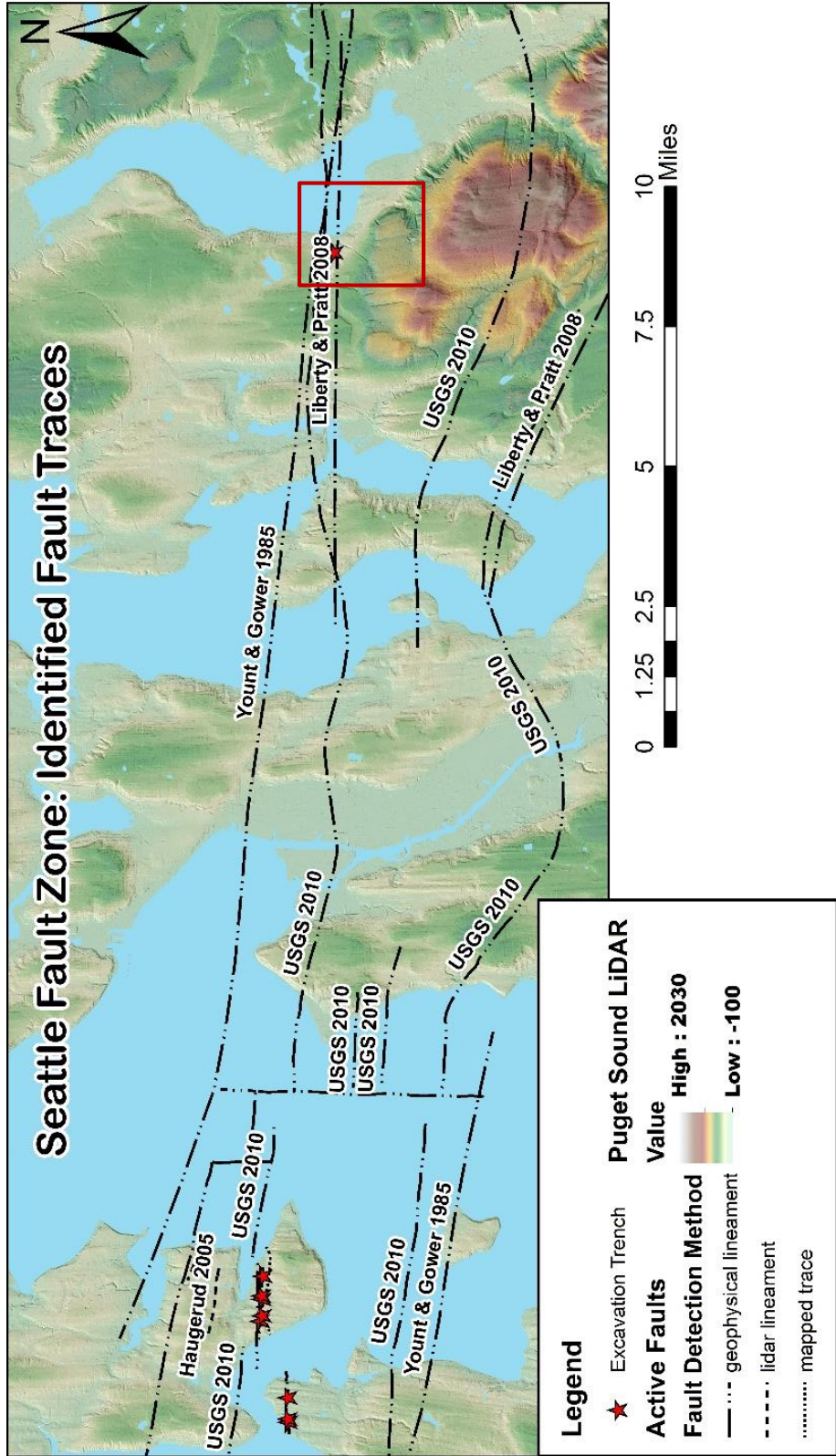


Figure 1. Identified fault traces within the Seattle Fault Zone. Red box indicates the study area. Data sources: Puget Sound LiDAR Consortium, WA DNR Fault database.

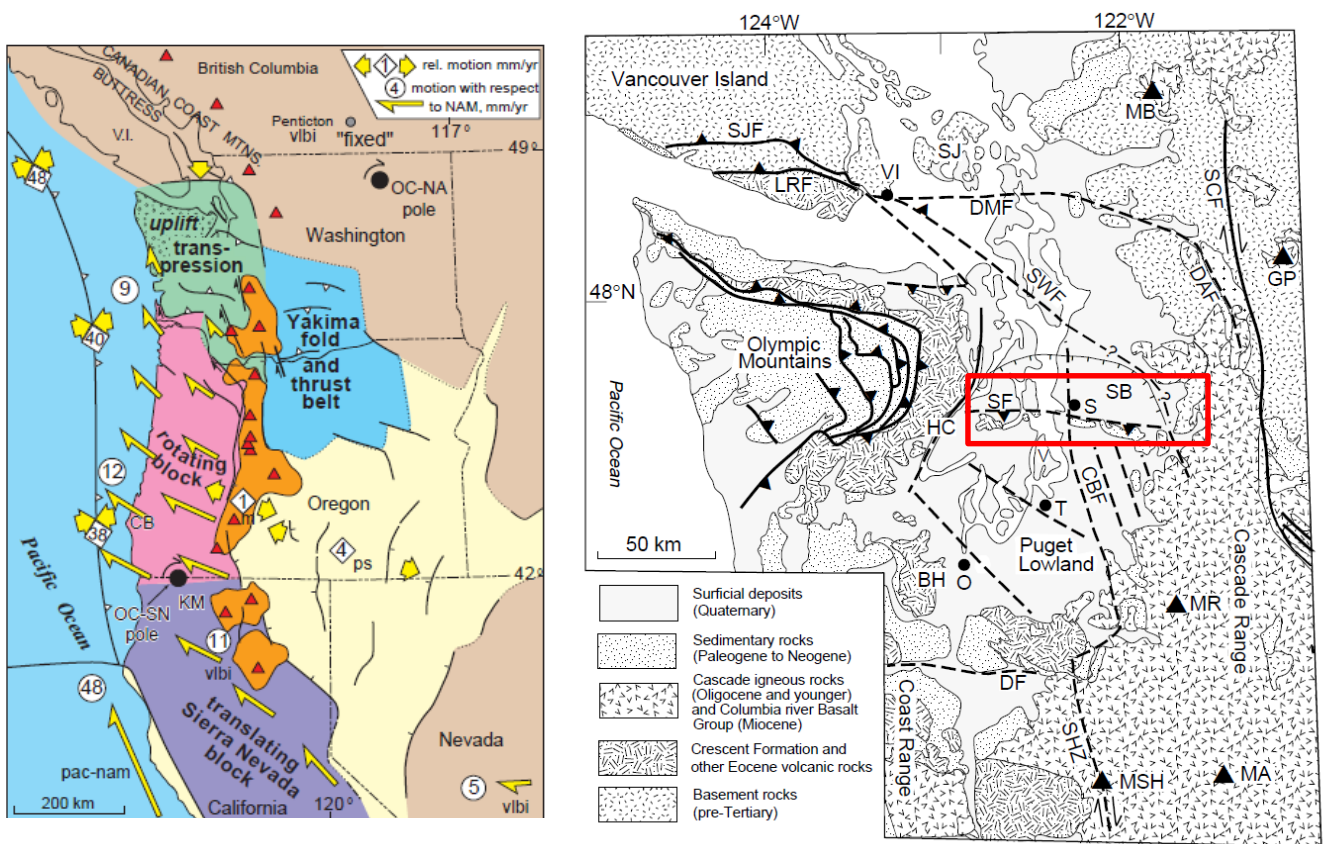


Figure 2. Depiction of the migrating Cascadia fore-arc including the Sierra Nevada, Oregon, and Washington blocks (left). Image taken from Wells et al. 1998. Crustal Faults of western Washington (right). Red box indicates the location of the Seattle Fault Zone. Figure taken from Johnson et al. 1999.

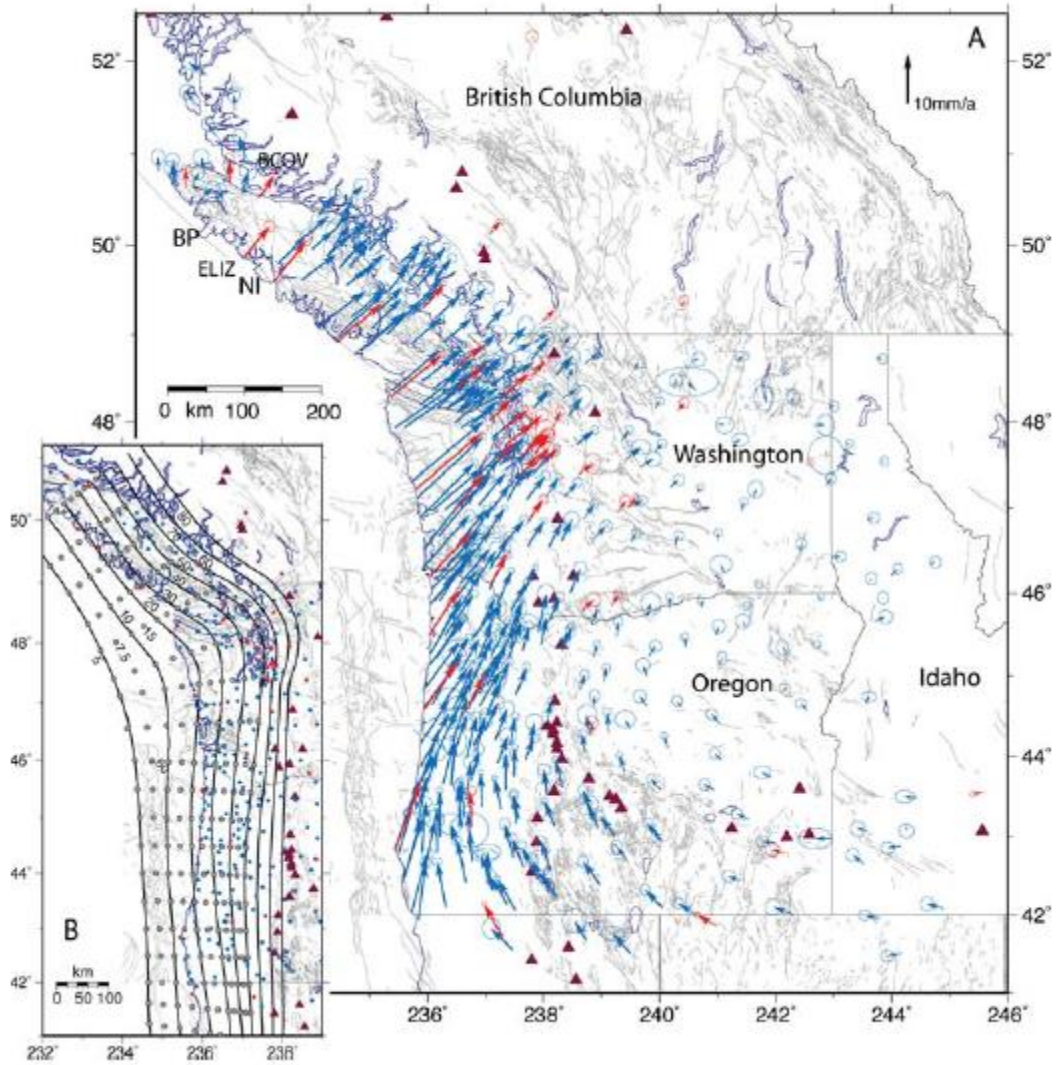


Figure 3. GPS velocity vectors illustrates crustal block rotation in the North American Plate. Red vector arrows are sourced from continuous vector data. Blue vector arrows are from survey mode sites. Triangles are locations of volcanoes. Figure taken from McCaffery et al., 2007.

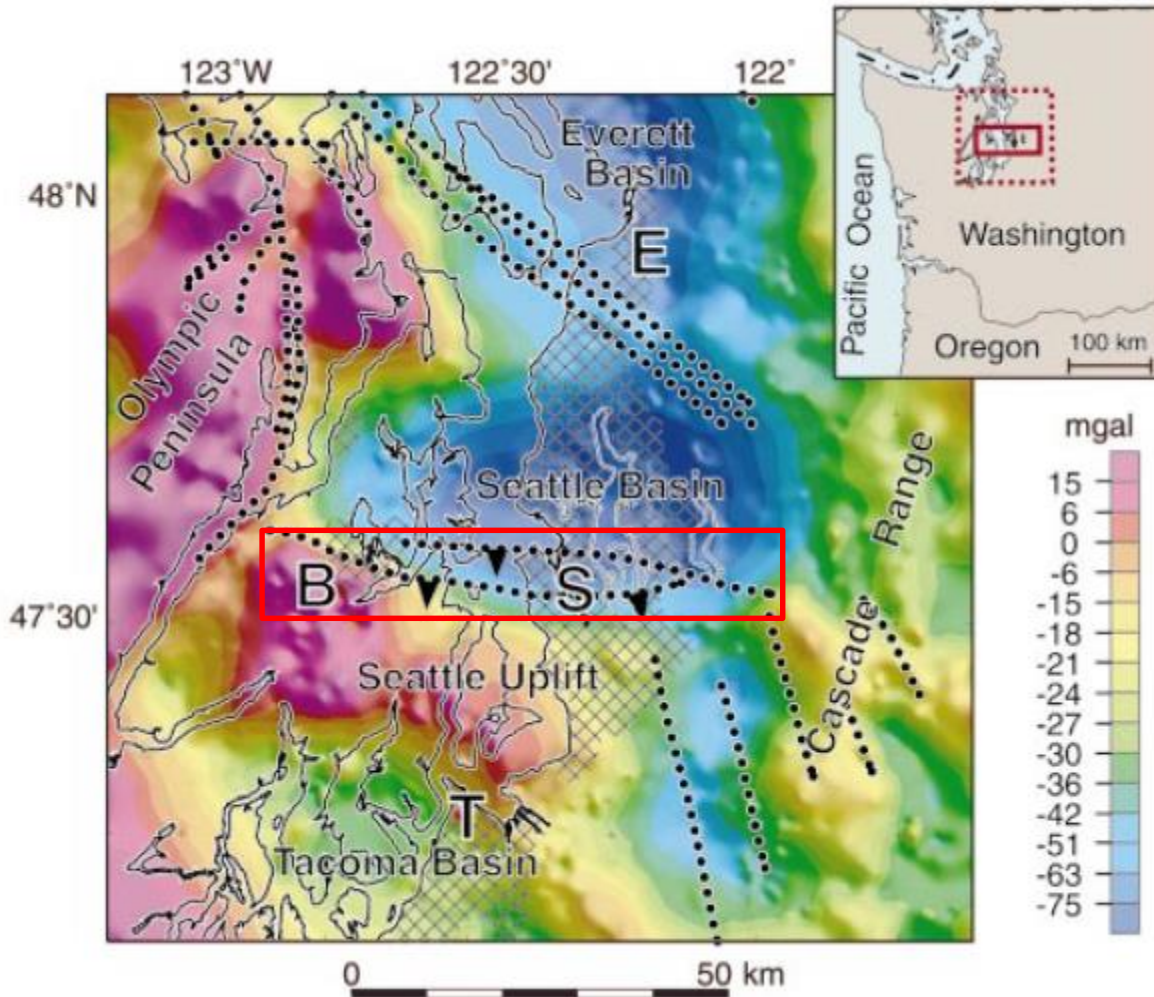


Figure 4. Gravity map depicting uplifts and basins of the Puget Lowland. Mapped faults are from Yount and Gower (1991) and Johnson et al. (1996). Red box delineates the extent of the Seattle Fault Zone from the Olympic Peninsula to the Cascade Range. Figure taken from Blakely et al. 2002.

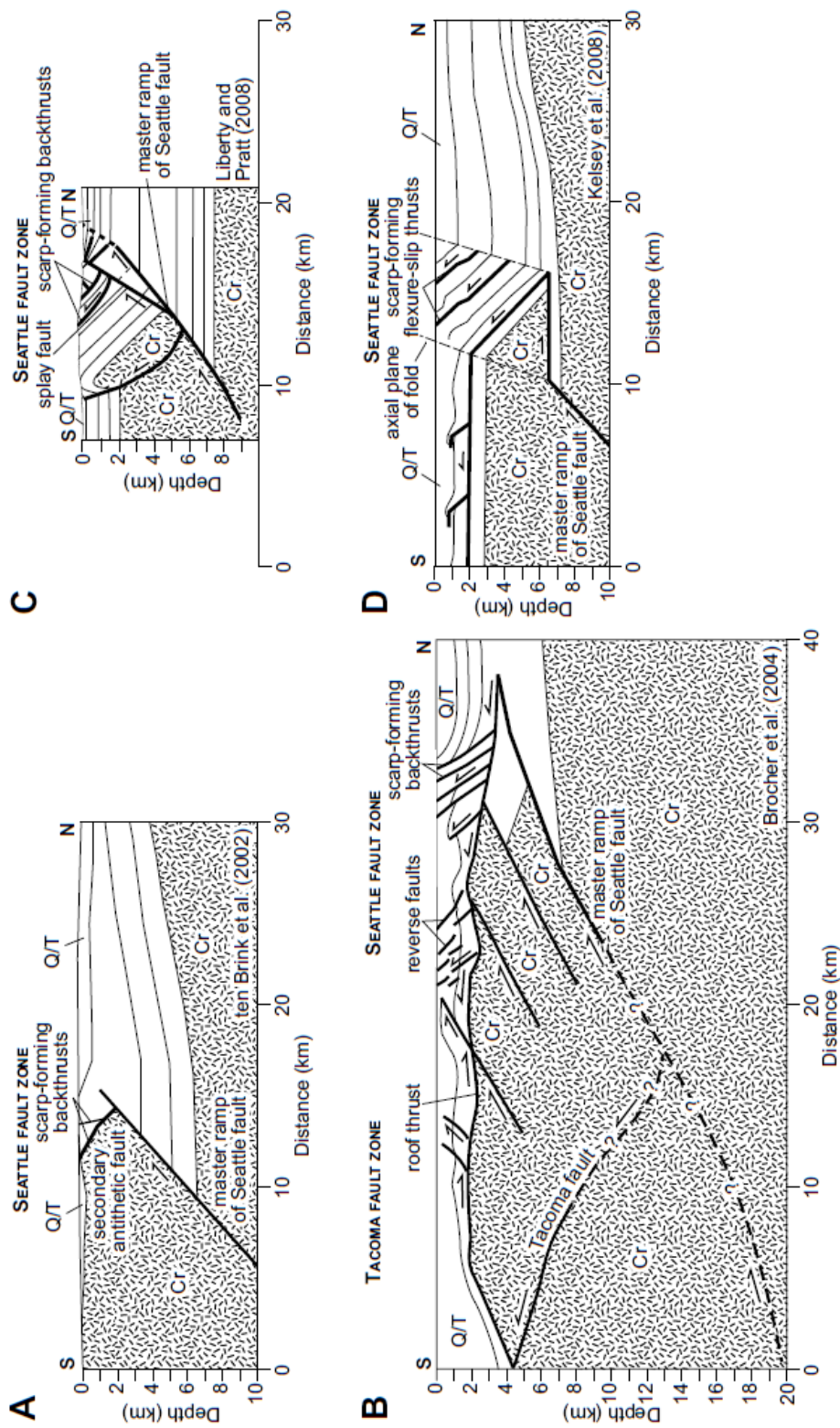


Figure 5. Illustration of the diverse fault models, Nelson et al. 2014.

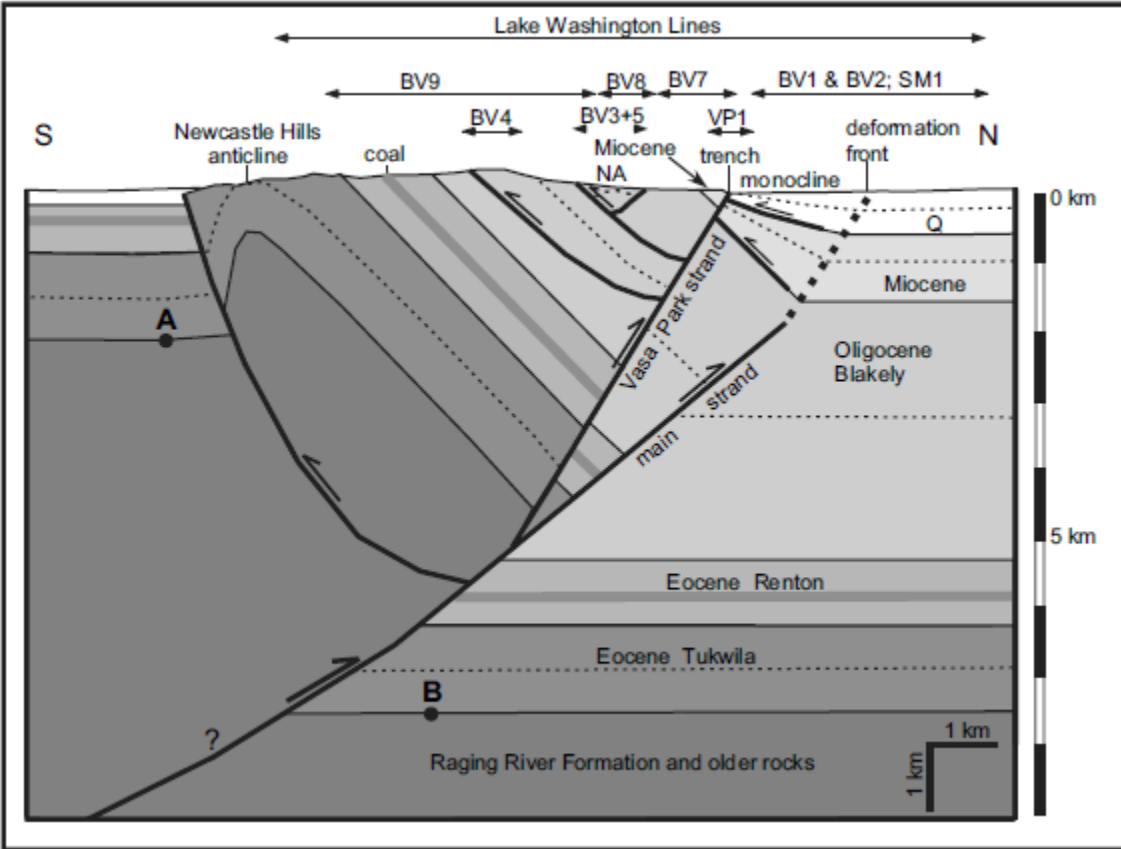


Figure 6. Seattle Fault model interpreted from seismic surveys through Bellevue, WA (Liberty and Pratt, 2008). Figure 30 illustrates the location of seismic lines BV1-9.

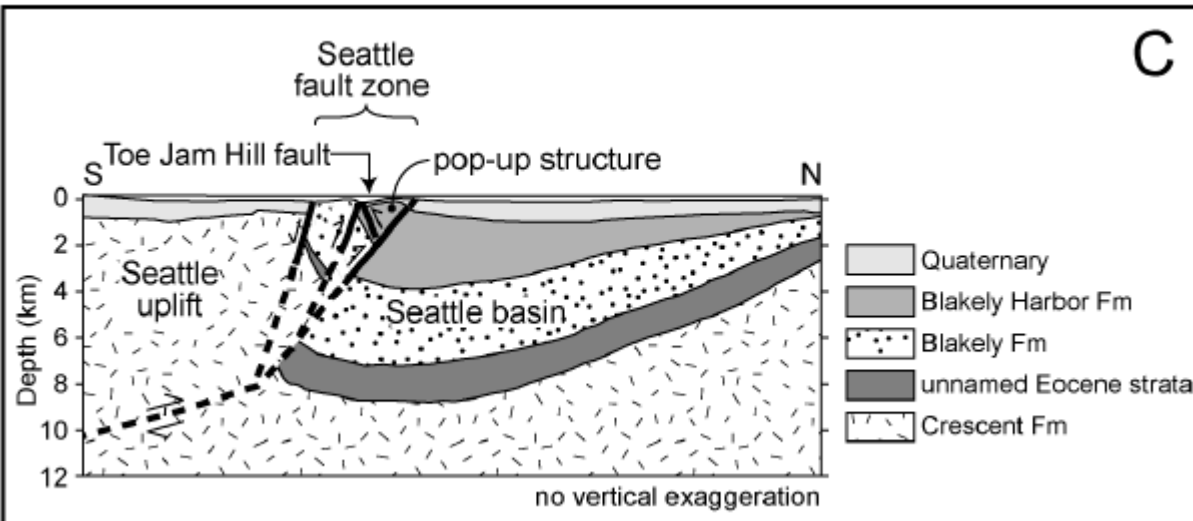


Figure 7. Seattle fault model of the western extent of the fault, interpreted from the Toe Jam Hill paleoseismic trench (Nelson et al., 2003).

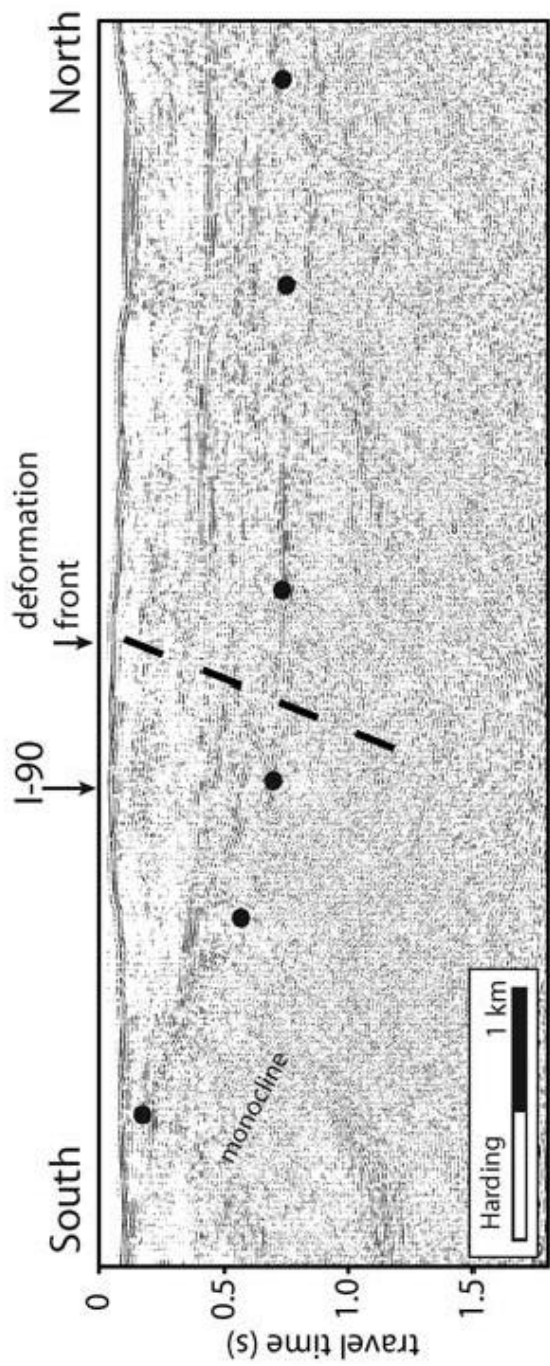


Figure 8. Harding et al. (1988) seismic survey through Lake Washington. Figure 30 shows the location of this seismic line. The Seattle monocline and the deformation front are illustrated.

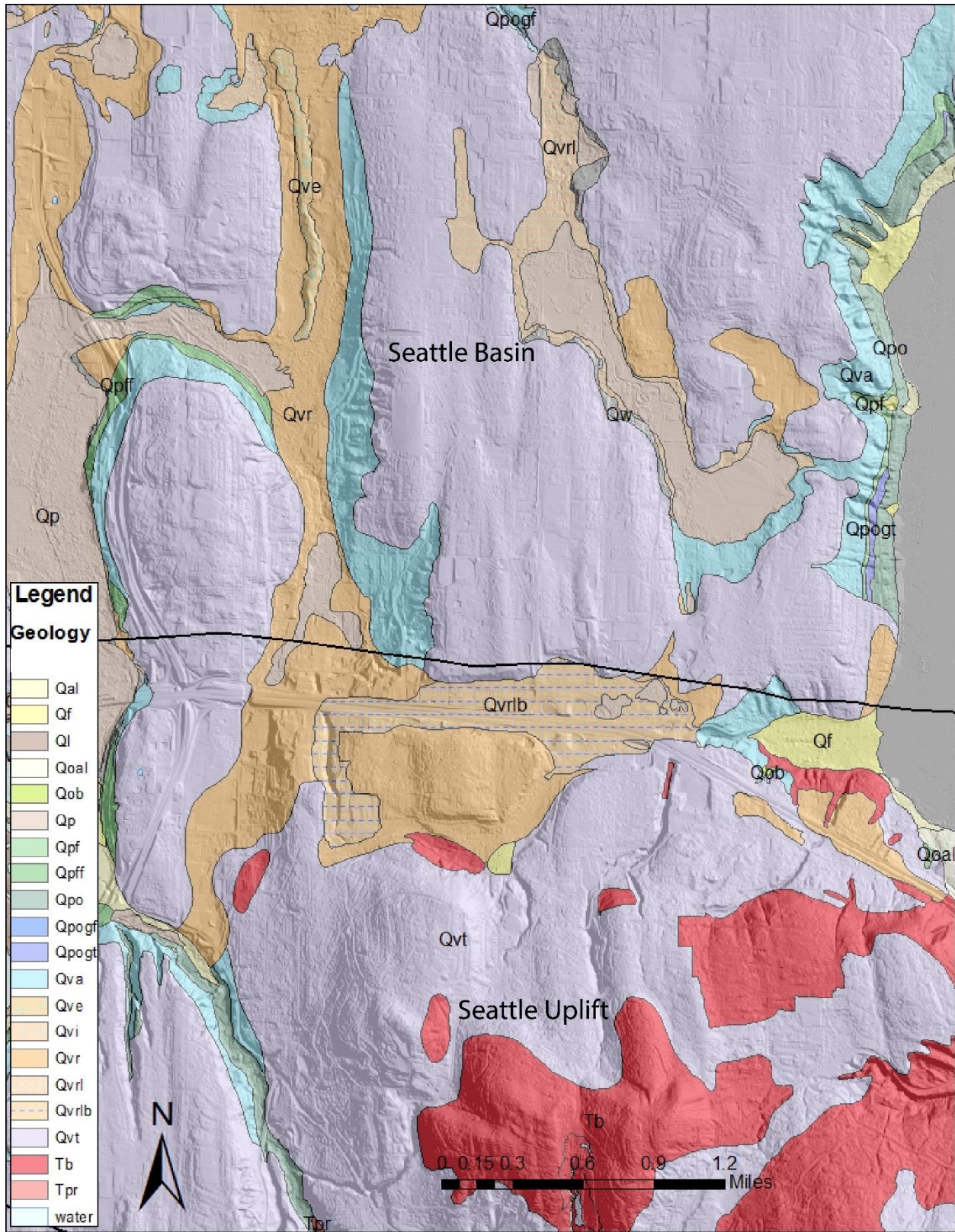


Figure 9. Geologic map of Bellevue, WA illustrating the portion of Seattle Uplift and the Seattle Basin that are part of or near the study area (Troost and Wisler, 2012).

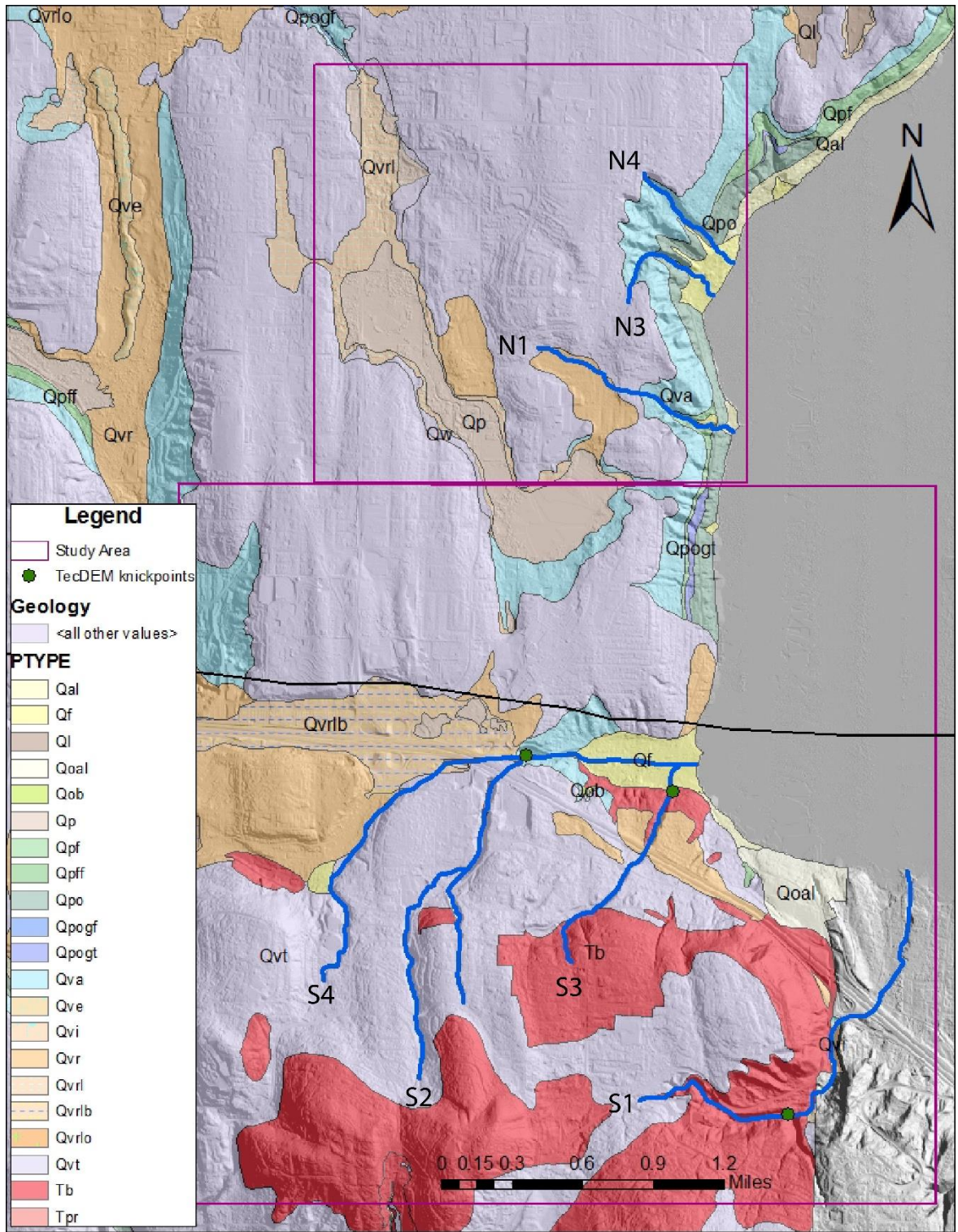


Figure 10. Geologic map of eastern Bellevue, WA (Troost and Wisner, 2012). Purple boxes delineate the two study areas used in the TecDEM stream analysis. The northern area is outside the fault zone and contains no knickpoints. See Figures 22-24 for analysis of streams N1, N3, N4. Green dots in the southern area represent the location of the knickpoints within the stream channels. See Figures 17-20 for analysis of streams S1, S2, S3, S4.

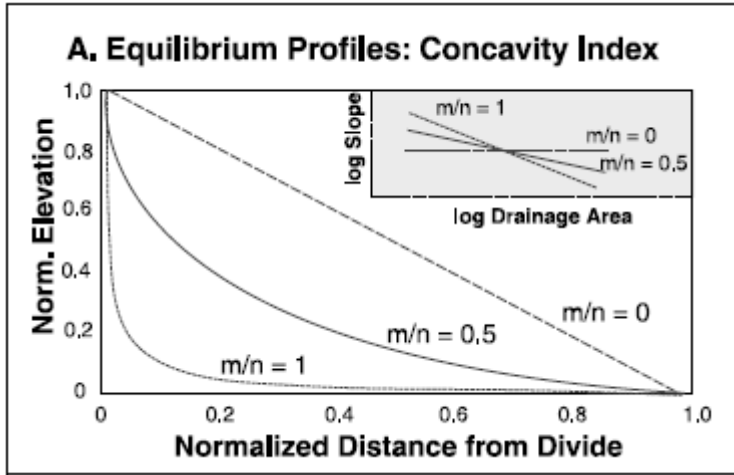


Figure 11. Solid line represents an equilibrium longitudinal profile. The ratio of m/n represents the stream profile concavity. M/n ratios greater than 0 represent higher concavity values. Figure taken from Duvall et al. 2004.

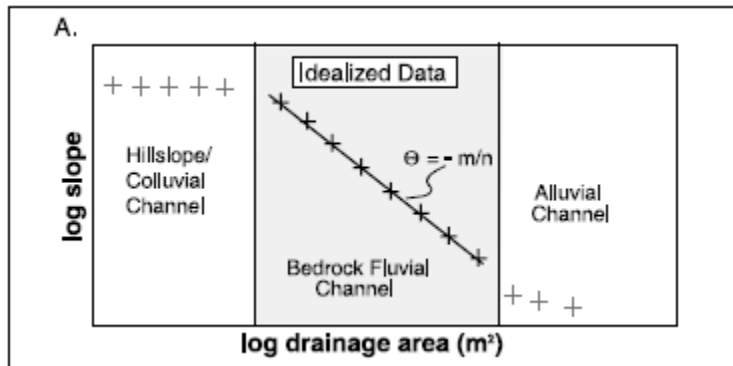


Figure 12. Slope vs. drainage area plot of a stream in equilibrium. There is a linear relationship between slope and drainage area in the fluvial channel. Figure taken from Duvall et al. 2004.

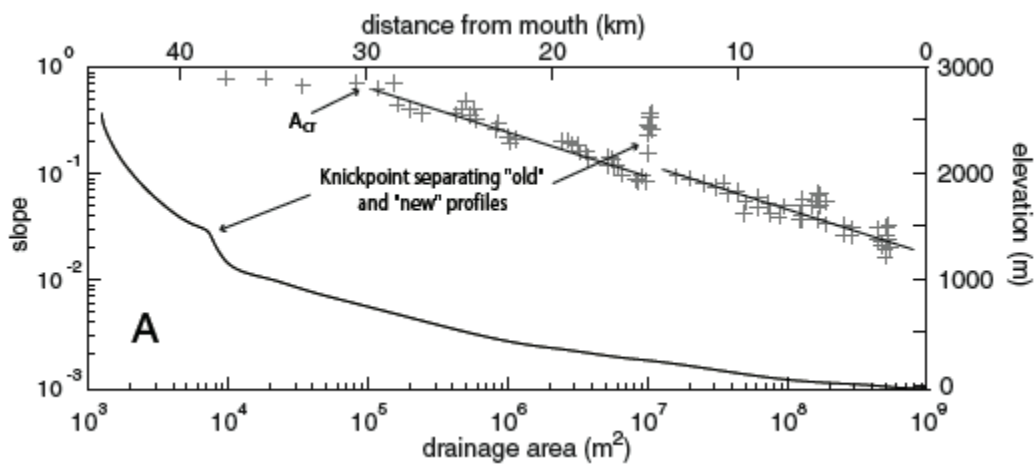


Figure 13. Figure illustrating a typical knickpoint along a graded stream profile. Figure taken from Wobus et al., 2006.

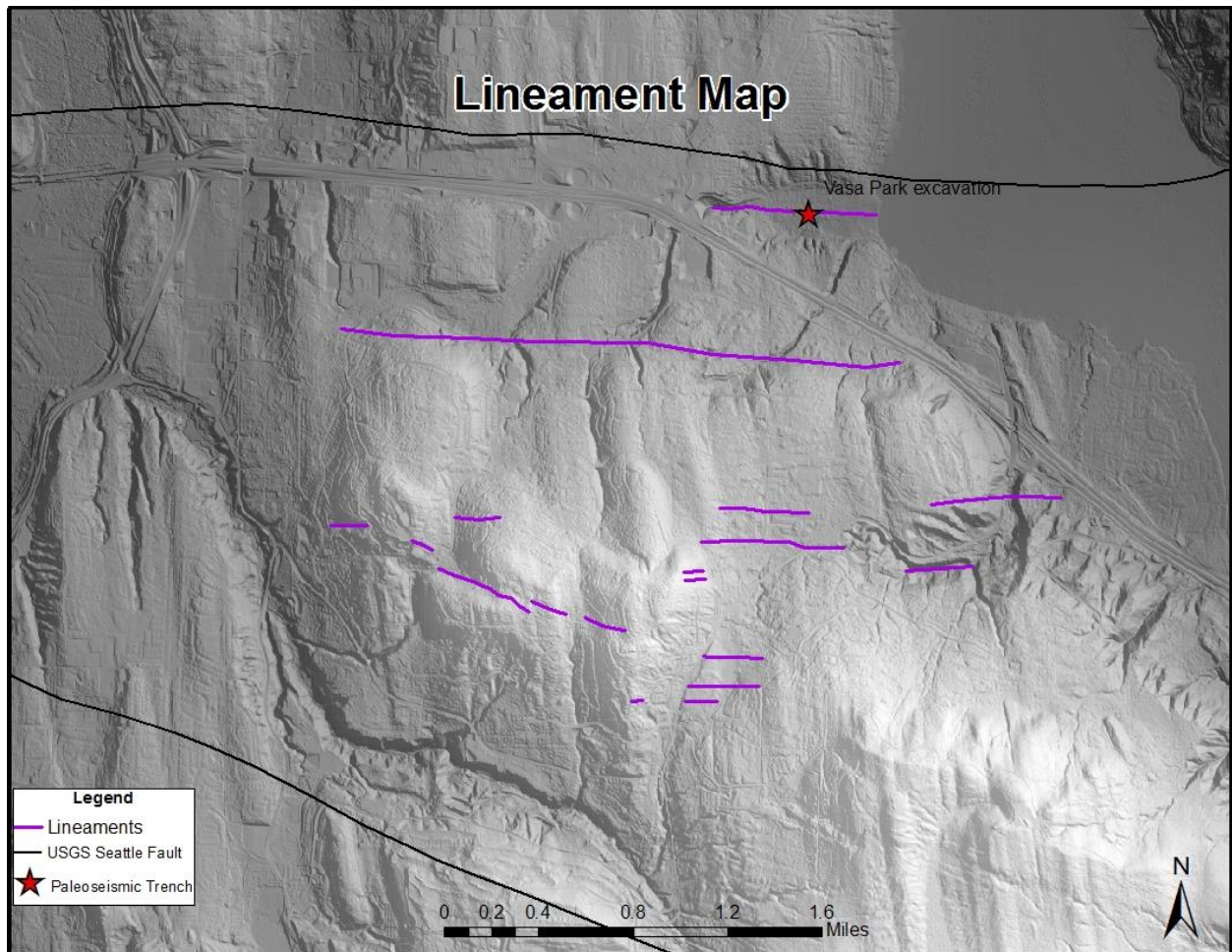


Figure 14. Lineament map illustrating the linear features in eastern Bellevue within the Seattle Fault zone. These are scarp-like features that aid in focusing fault investigations. Linear features in the southeast corner of the map were not included in this map because this study focuses on the northern extent of the fault zone. Data sources: PSLC LiDAR and WA DNR fault database.

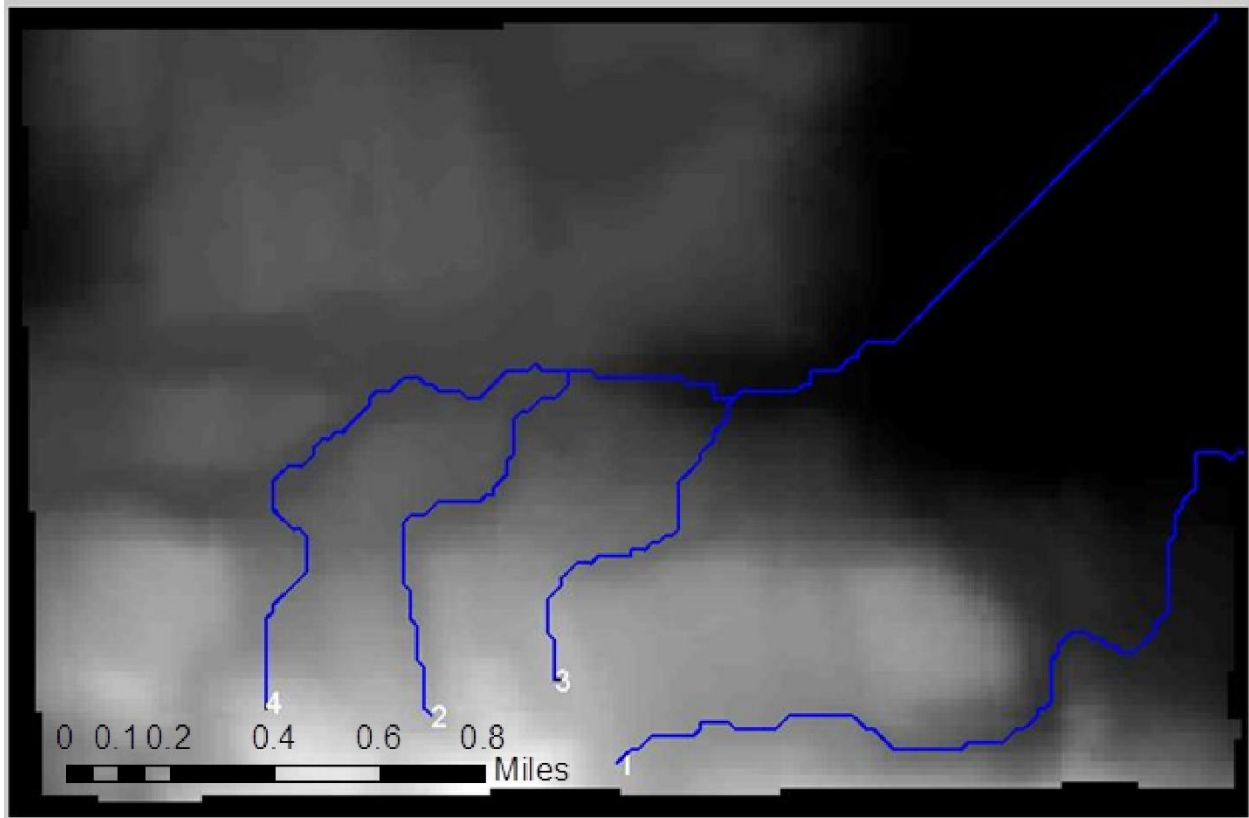


Figure 15. Digital elevation model generated in TecDEM used for stream profile analysis (Shazhad and Gloaguen, 2010). Streams of interest are labeled. Figures 16-17 are the resulting plots.

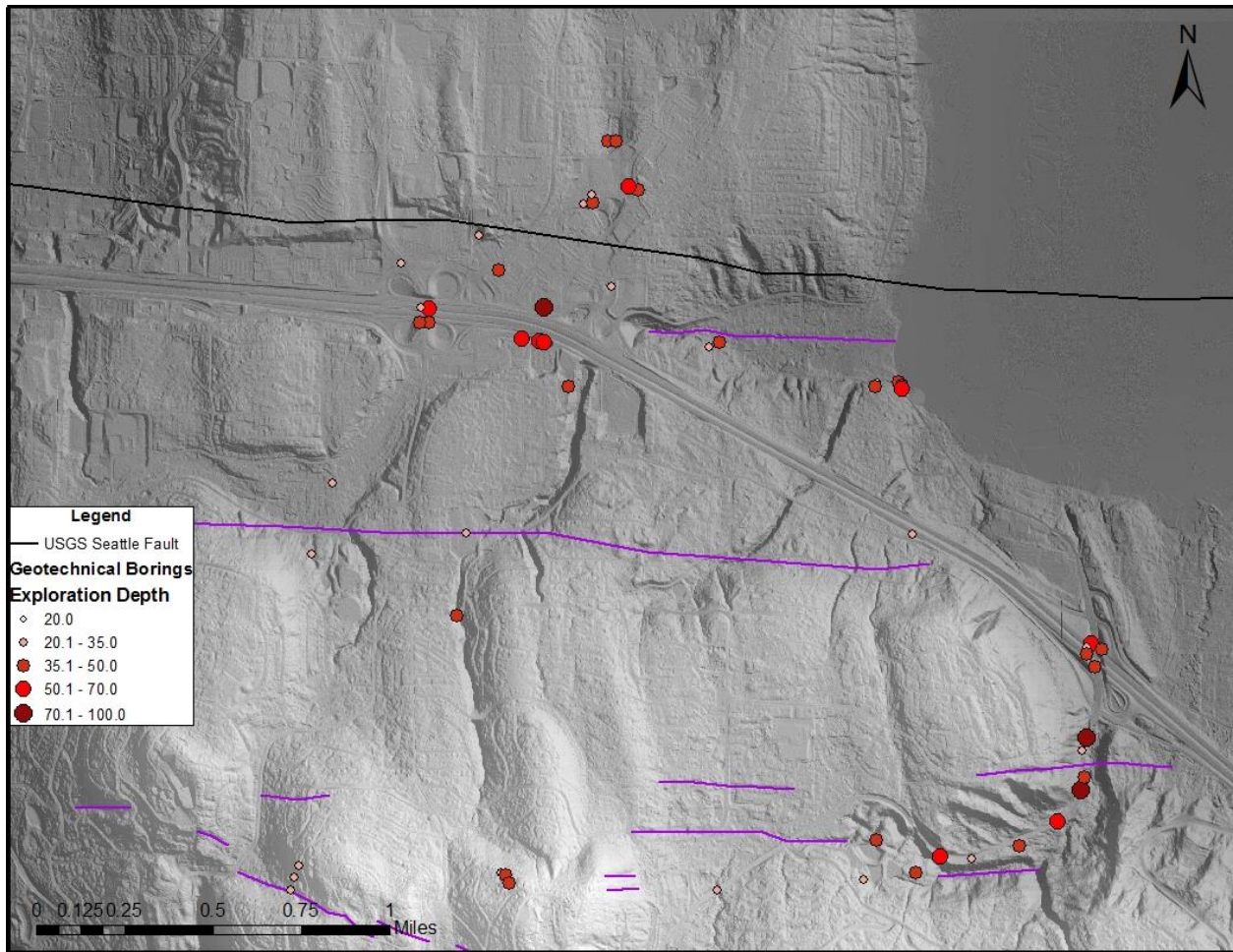


Figure 16. Selection of deep geotechnical borings in the study area that were selected for their high level of detail. Borings overlaid onto low angle illumination LiDAR with observable lineaments helps to guide subsurface borehole investigations.

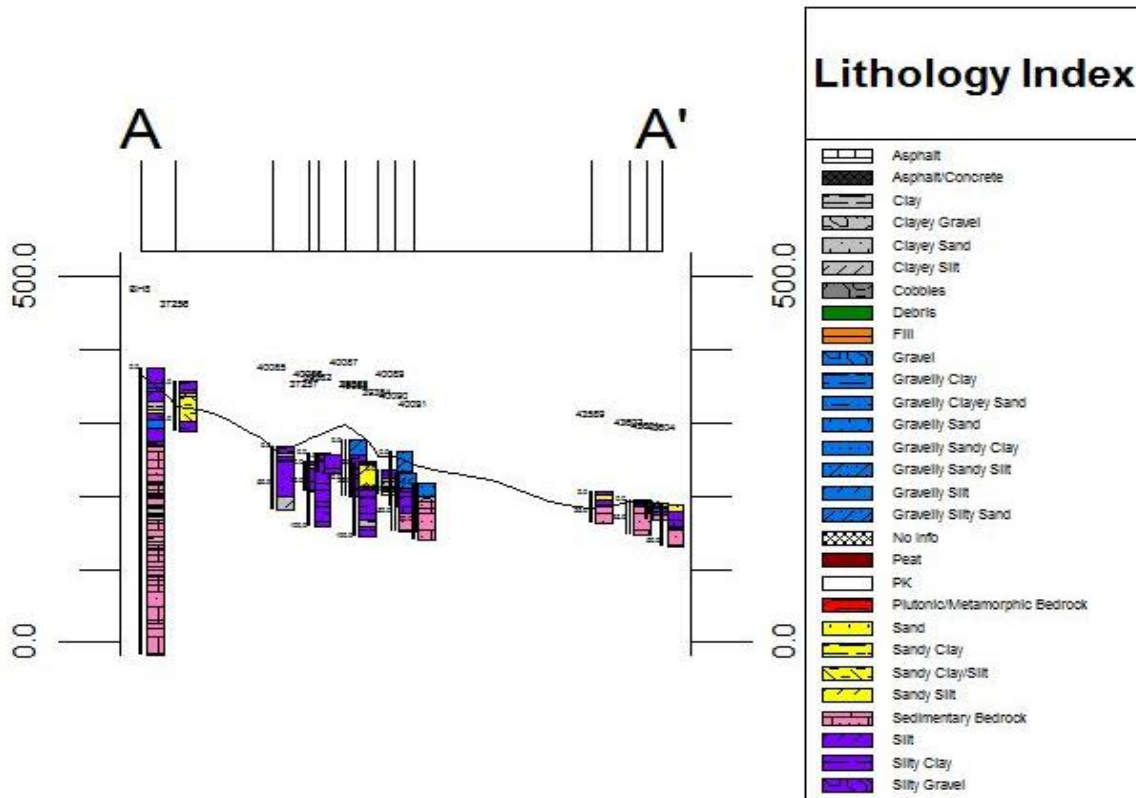
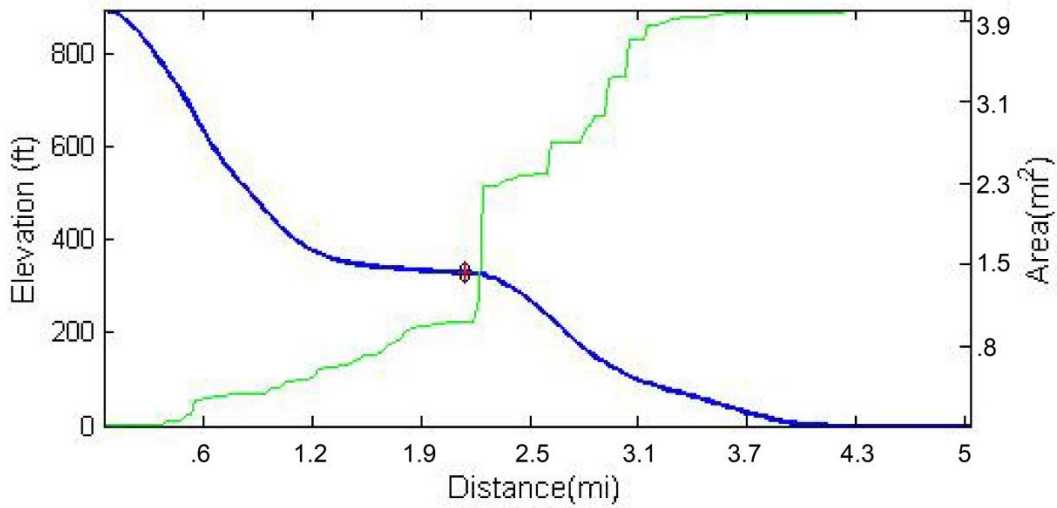


Figure 17. Example Rockworks figure of a swath profile. This figure is difficult to read and poorly constructed.

Longitudinal and Area Profile for Stream No. S4



Slope-Area Data for Stream No. S4

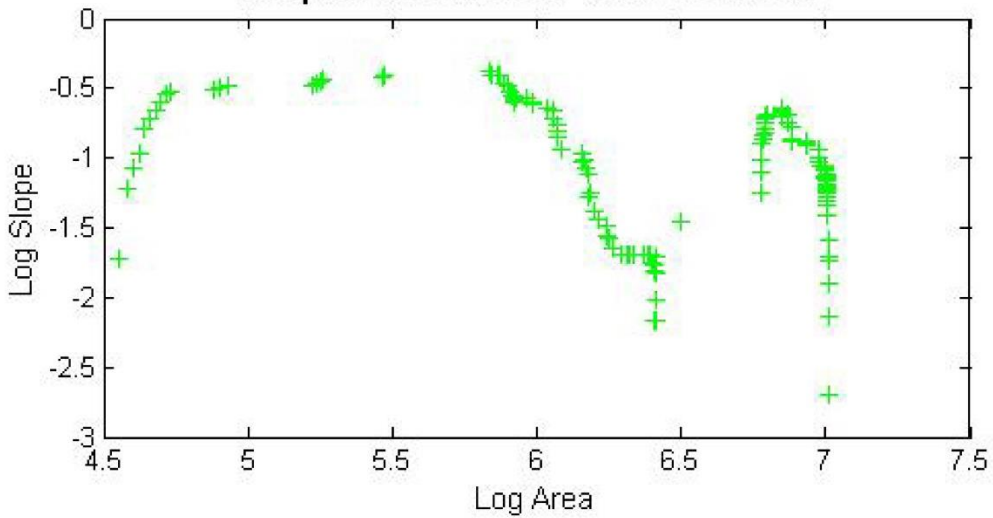


Figure 18. Longitudinal profile and slope-area plot for stream S4. Blue line is the longitudinal profile, the red dot indicates the location of the knickpoint. Refer to Figures 14 and 10 for the location of stream 1. On the slope-area graph, the zone with sparse data between 6.5 and 6.8 represents a knickzone which is a transitional zone within the stream channel.

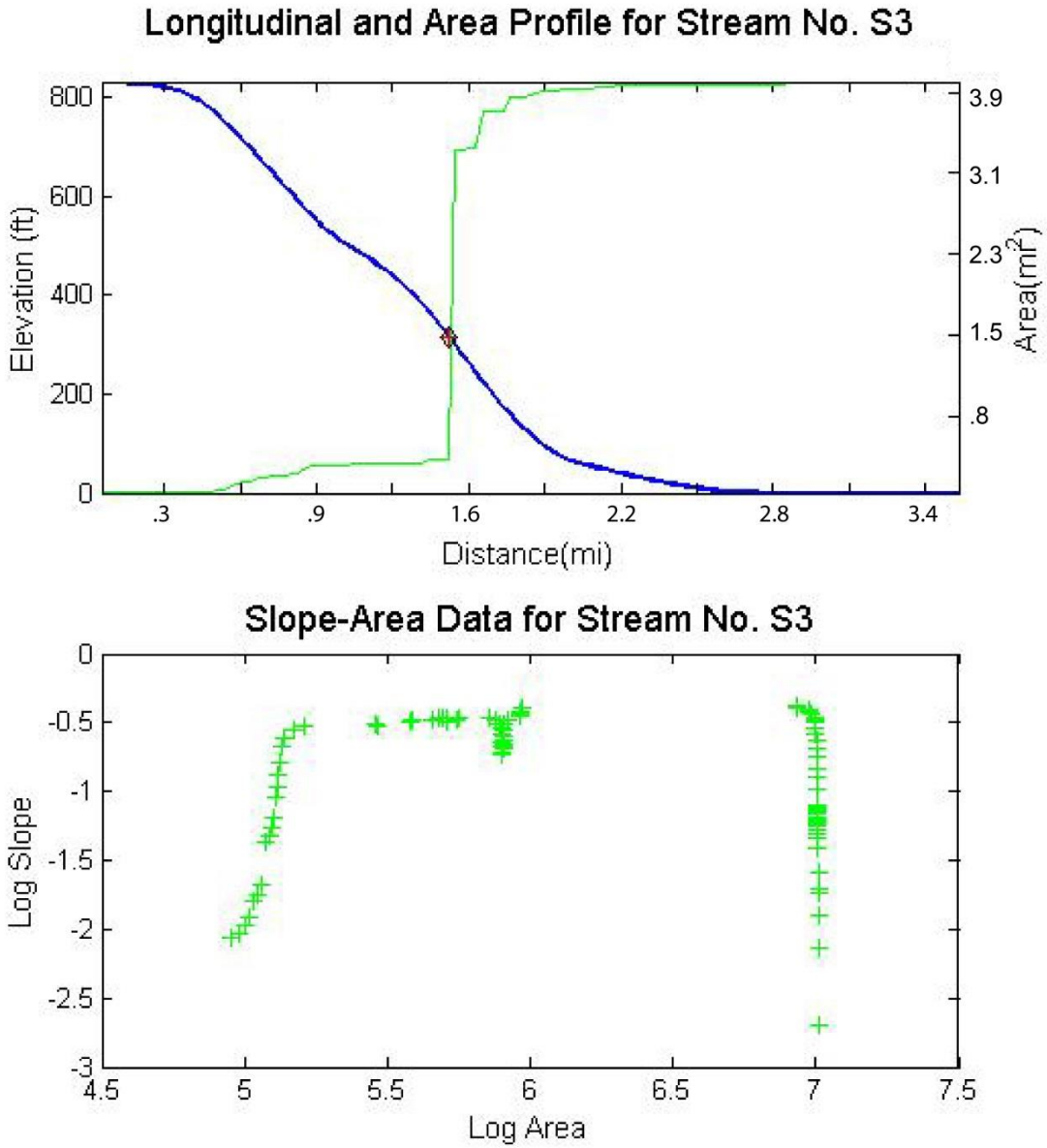
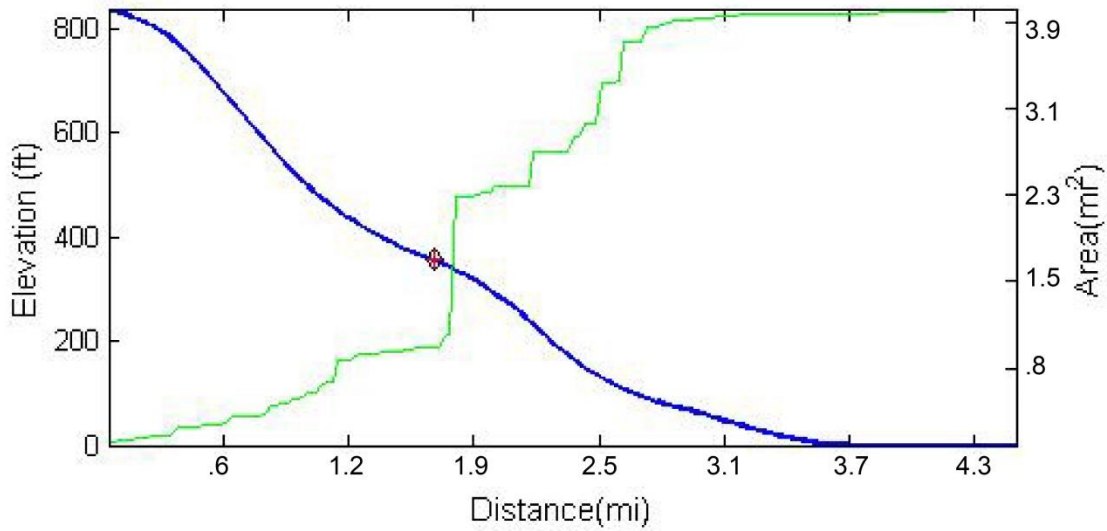


Figure 19. Longitudinal profile and slope area plot for stream S3. Red dot indicates the location of the knickpoint. Refer to Figures 14 and 10 for stream locations. A knickzone is identifiable from 6-7 on the slope-area graph.

Longitudinal and Area Profile for Stream No. S2



Slope-Area Data for Stream No. S2

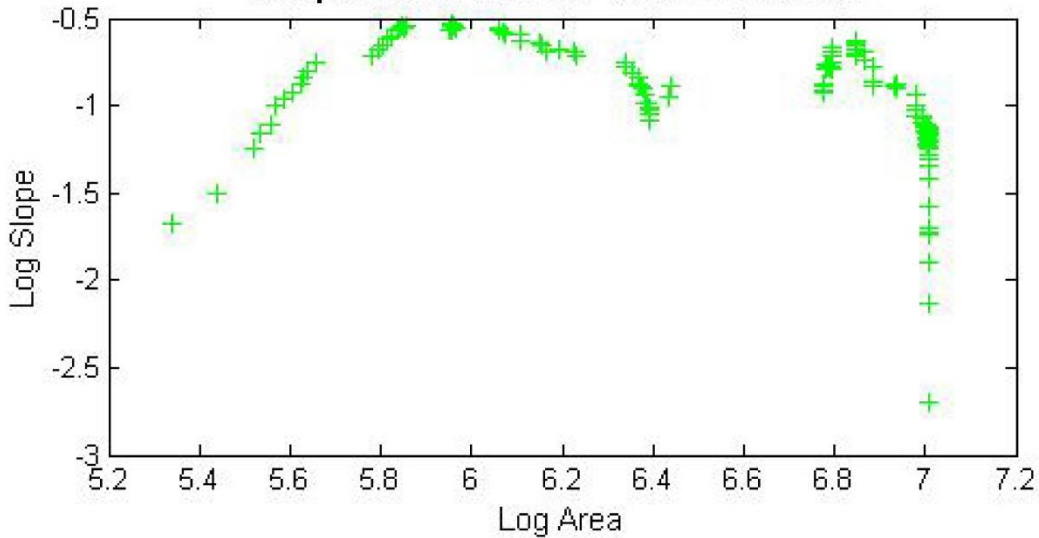
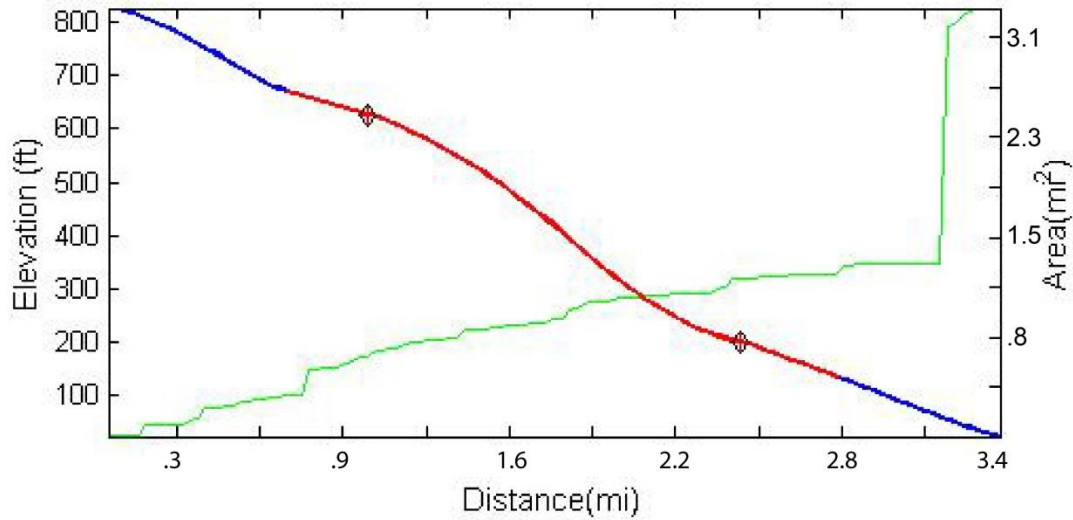


Figure 20. Longitudinal profile and slope area plot for stream S2. This plot shows a knickpoint indicated as the red dot along the longitudinal profile (blue line). Refer to Figures 14 and 10 for the location of stream 4. The slope area plot has sporadic data because this stream is small and the basin area is low. The knickzone lies between 6.4 and 6.7 on the slope-area graph.

Longitudinal and Area Profile for Stream No. S1



Slope-Area Data for Stream No. S1

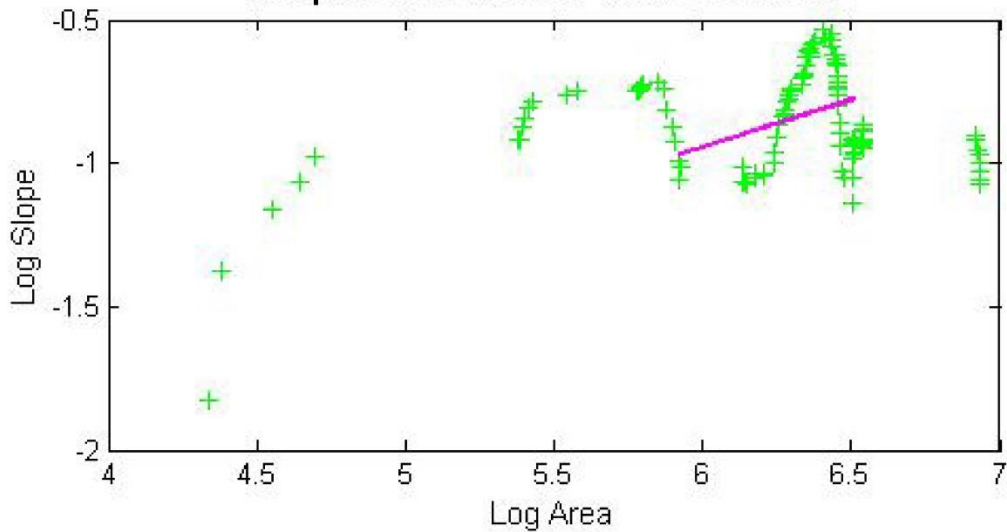


Figure 21. Longitudinal profile and slope area plot for the stream that crosses the identified fault. Red dots indicate the location of knickpoints. Refer to Figures 14 and 10 for stream locations. There are two knickzones on the slope-area graph. One can be found from 5.8-6 and the other lies between 6.3 and 6.5. The knickzone from 5.8-6 can be found upstream of the hypothesized fault.

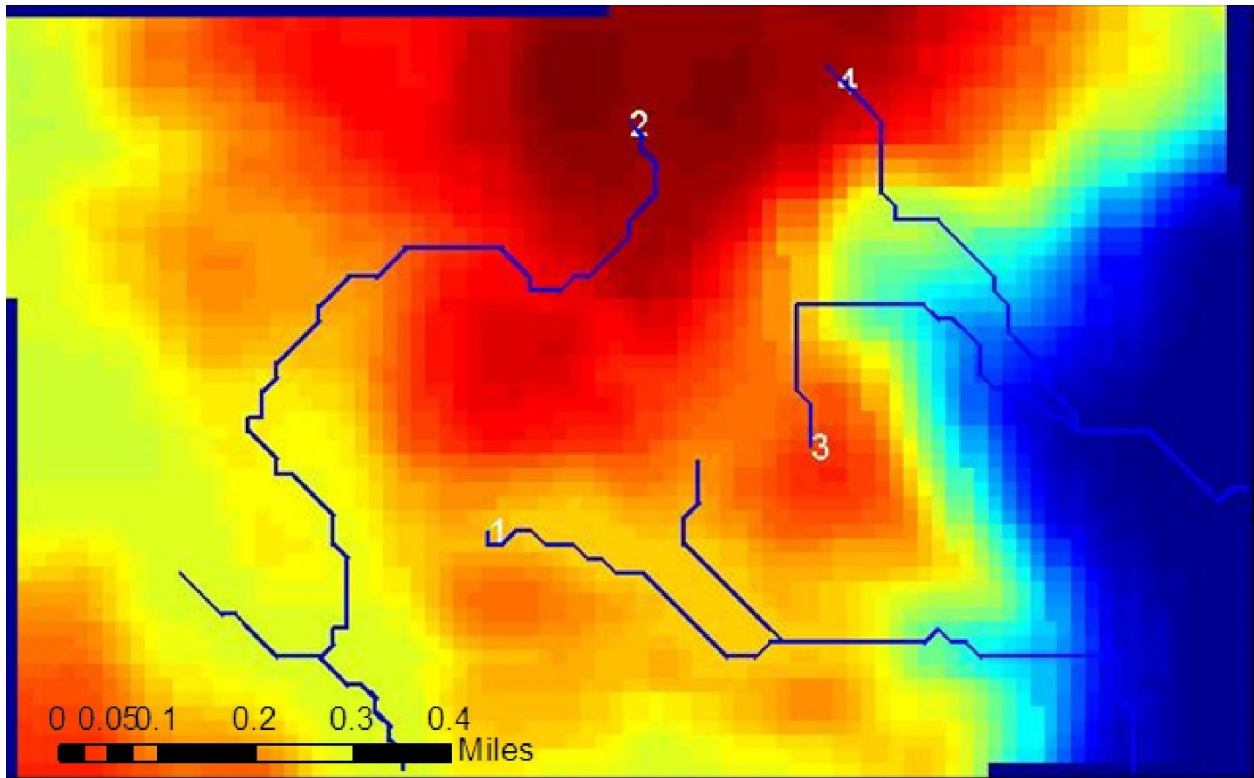


Figure 22. DEM and stream channels generated in TecDEM for the northern area. Refer to Figure 10 for the extent of this DEM.

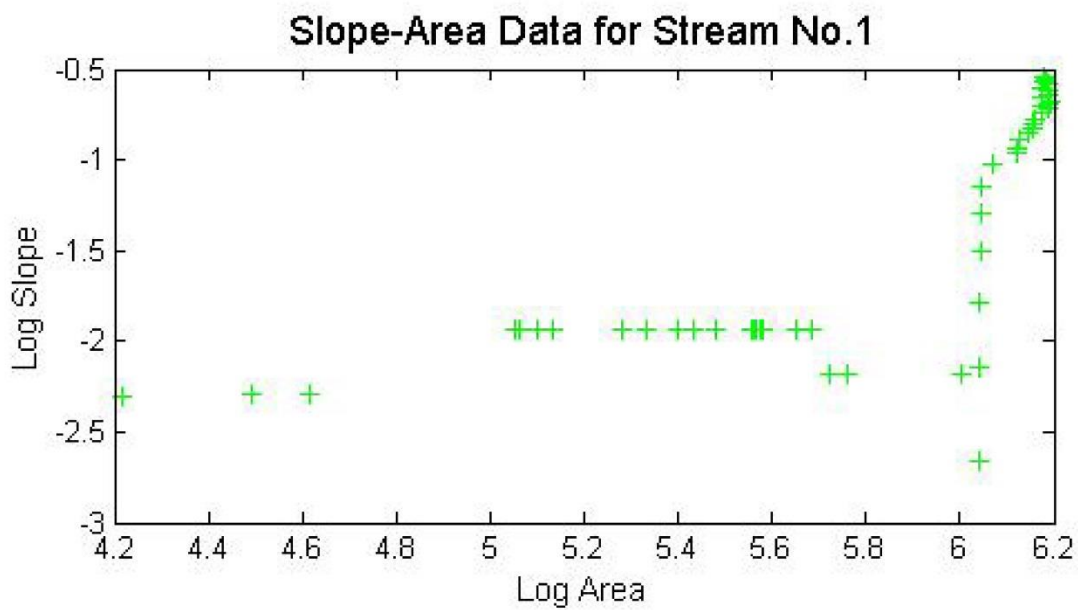
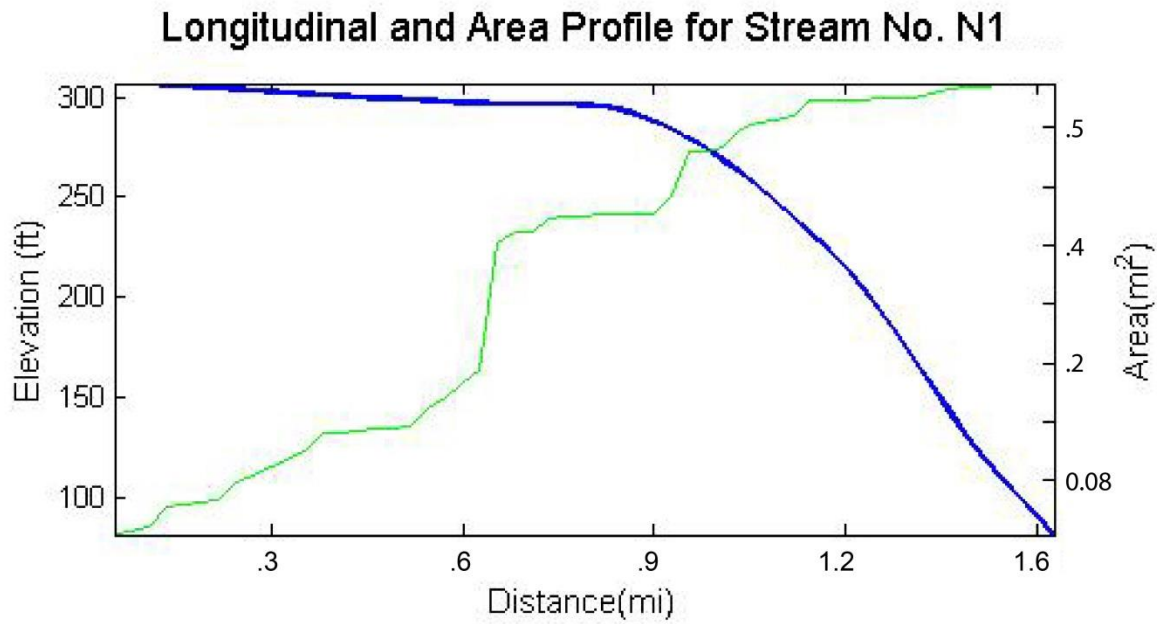


Figure 23. Slope area data and longitudinal profile for stream N1. Refer to Figure 22 and 10 for stream location.

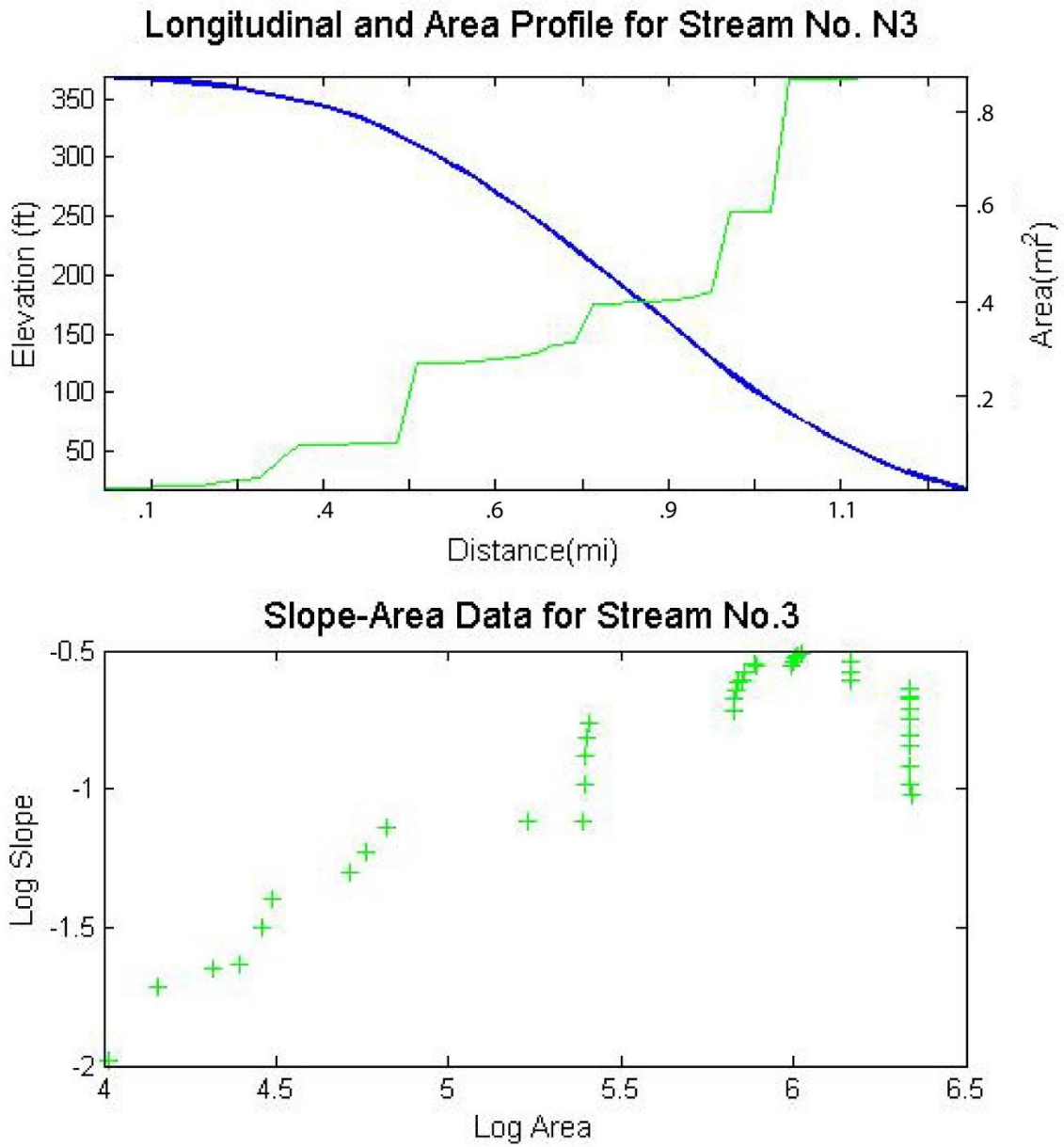
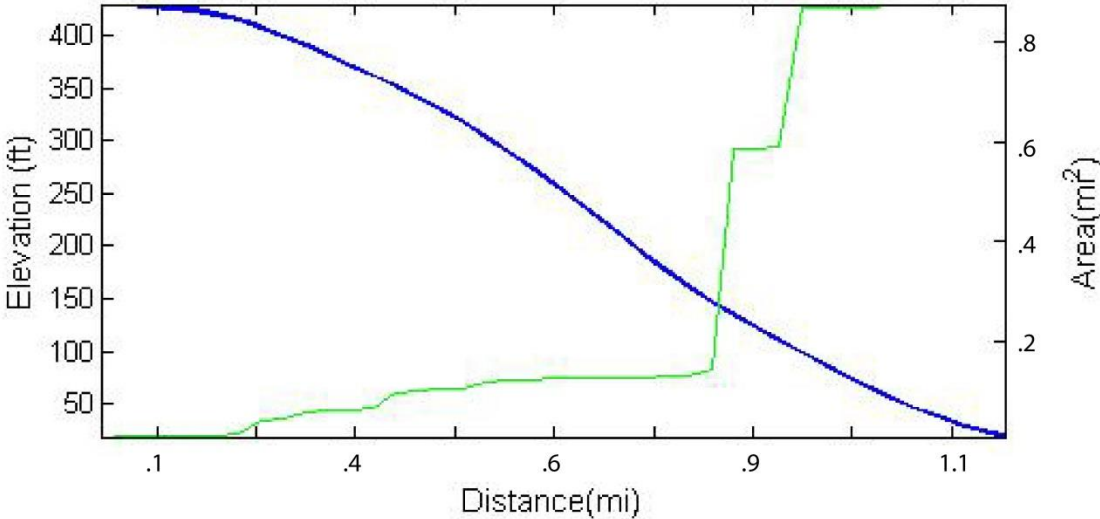


Figure 24. Slope area data and longitudinal profile for stream N3. Refer to Figure 22 and 10 for stream location.

Longitudinal and Area Profile for Stream No. N4



Slope-Area Data for Stream No.4

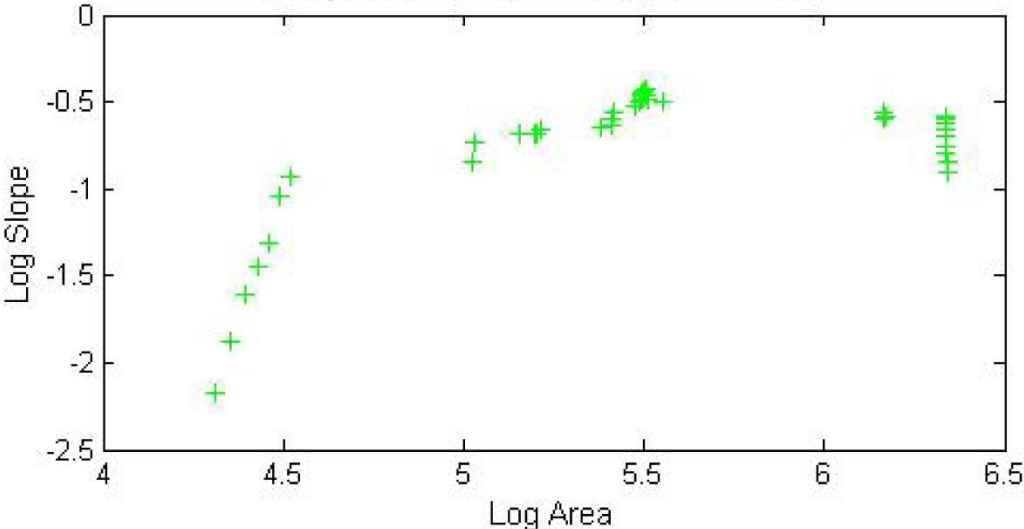


Figure 25. Slope area data and longitudinal profile for stream N4. Refer to Figure 22 and 17 for stream location.

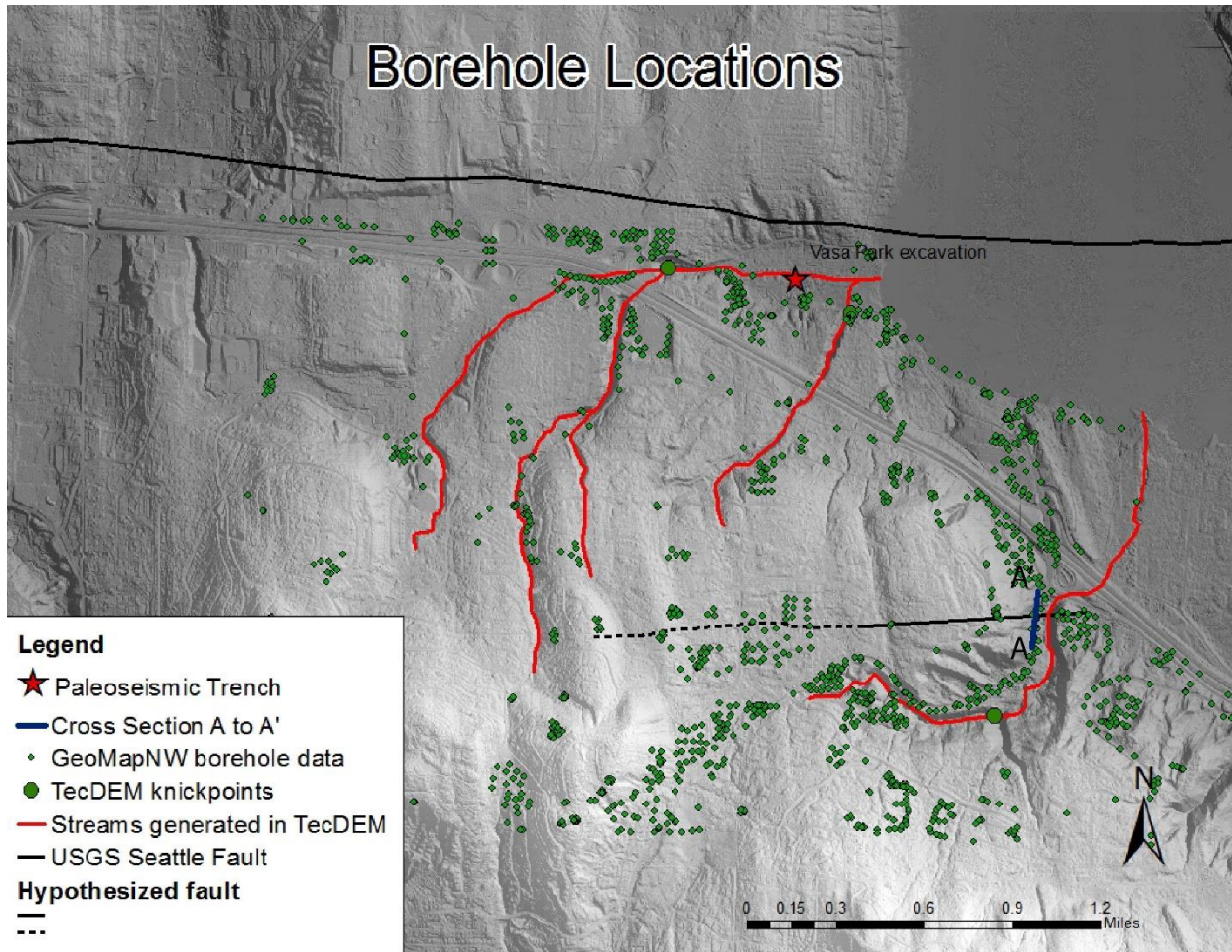


Figure 26. Borehole locations map. These are the borings selected to analyze in this study. Cross section A to A' is indicated with the blue line.

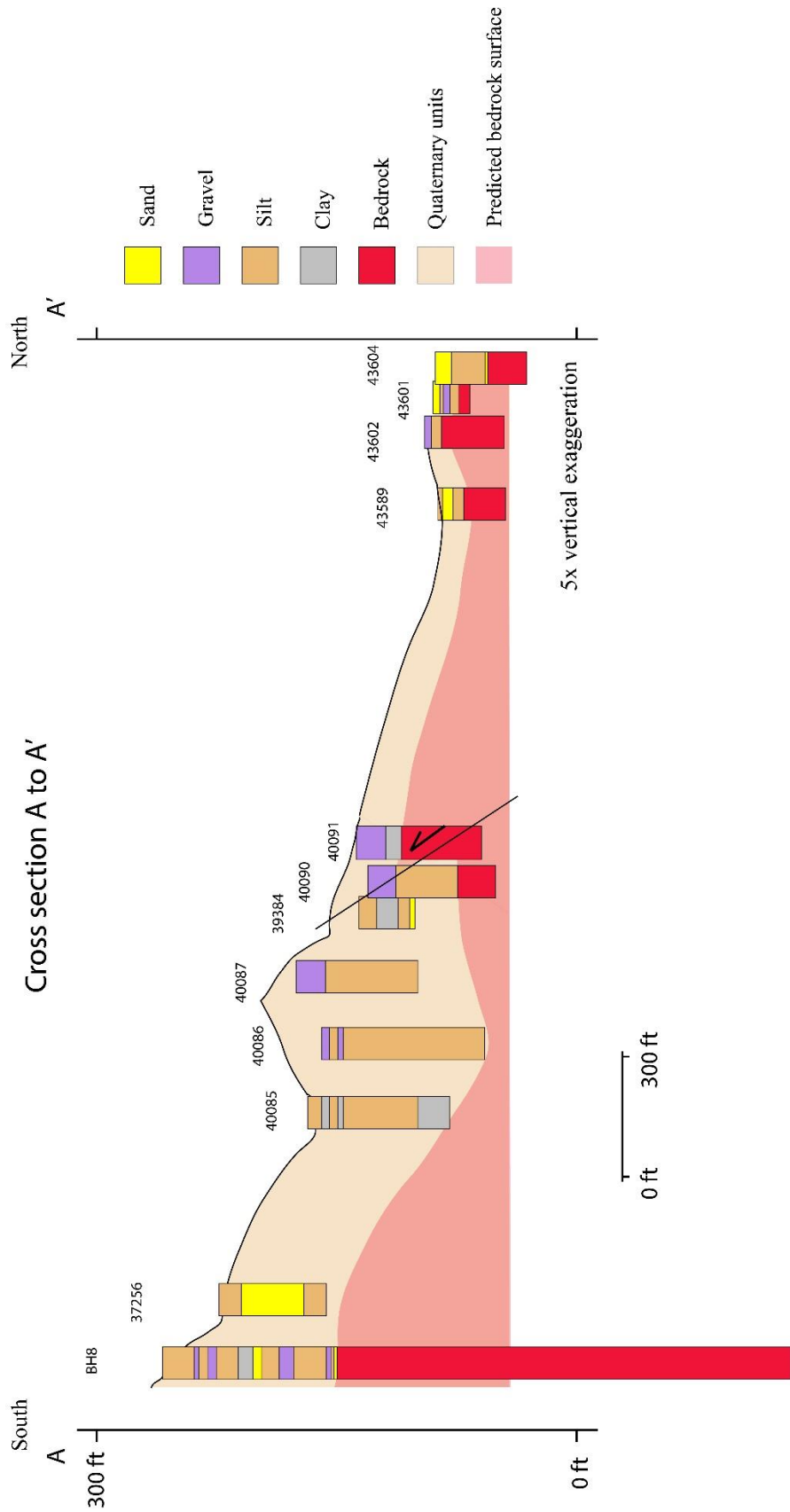


Figure 27. Simplified cross section showing proposed fault offset. Borehole strip logs plotted against a topographic profile show a vertical offset in bedrock between borings 40090 and 40091. This offset has a north-side-up motion which is consistent with Liberty and Pratt's (2008) seismic data. See Figure 27 for the location of A to A'. See Table 1 for boring logs containing evidence consistent with faulting.

Table 1. Layer descriptions for those borings that contain fault evidence across the identified offset in Cross Section A to A'. Refer to Cross Section (Figure 27, 28) for the location of these borings.

Exploration ID	Layer top depth (ft.)	Layer bottom depth (ft.)	Layer Description	Exploration Depth (ft.)
39383	0.0	31.0	Loose to medium dense, gray-brown and iron stained, slightly clayey, silty, fine to coarse SAND with variable amounts of fine to coarse gravel and scattered cobbles	49.50
	31.0	34.0	Stiff, gray, fractured and slickensided , clayey SILT	49.50
	34.0	35.0	Medium dense, dark green-gray, silty, fine to coarse gravelly, fine to coarse SAND	49.50
	35.0	49.5	Hard, light brown to gray, silty CLAY with numerous sand partings at about 15 degree dip and a few thin layers of clean, fine sand	49.50
40087	0.0	19.5	Very loose to medium dense, dark brown to brown, gravelly, sandy SILT to gravelly, silty SAND, moist to wet, scattered to abundant siltstone and sandstone clasts (slide debris) ML to SM	76.00
	19.5	38.0	Loose to medium dense, silty, sandy GRAVEL, wet, sandstone clasts in a silty sand matrix, blue-gray below 31.4 feet, (slide debris) SM to GM	76.00
	38.0	51.5	Hard, gray, silty CLAY to clayey SILT, moist, laminated to layered with silt partings space 1/4-1/2 inch, (glaciolacustrine) CL to ML	76.00
	51.5	68.0	Very dense, green-gray to gray, clayey, silty, sandy, fine GRAVEL to silty, gravelly SAND, moist to wet, subangular green sandstone clasts and rounded to subrounded glacial gravel, scattered volcanics, disturbed texture, scattered zones of slickensided c	76.00
	68.0	76.0	Hard, gray, silty CLAY, moist, massive, trace slickensides (glaciolacustrine) CH	76.00
40091	0.0	18.5	Very loose, brown to green-gray, slightly gravelly to gravelly, silty SAND; moist to wet; clasts are primarily subangular sandstone with scattered rounded glacial gravel, scattered organics; (Colluvium or Slide Debris) SM.	77.90
	18.5	25.1	Dense, gray, clayey, silty, sandy GRAVEL to slightly clayey, slightly fine gravelly, silty SAND, trace organics; moist to wet; rounded; (Slide Debris) GC to SM.	77.90
	25.1	34.4	SANDSTONE: weak to very weak, gray-brown, fine-grained; closely jointed.	77.90
	34.4	77.9	TUFF BRECCIA : weak, gray-brown, slightly weathered; closely jointed.	77.90
39384	11.0	16.0	Hard, gray-brown and iron stained, clayey SILT with a trace of fine sand	34.40
	16.0	23.5	Very stiff, gray, clayey SILT with a trace of fine sand and tan laminations near 23.5 feet	34.40
	23.5	26.0	Very stiff, gray, silty CLAY with a fractured waterbearing zone 4 inches thick at 23.5 feet	34.40
	26.0	31.0	Dense, dark green-gray, silty, fine to medium SAND with a trace of coarse sand and fine gravel	34.40
	31.0	33.5	Hard, gray, clayey, fine sandy SILT with claystone fragments	34.40
	33.5	34.4	Very soft, dark green-gray, severely weathered SANDSTONE with slickensides at 33.5 feet	34.40

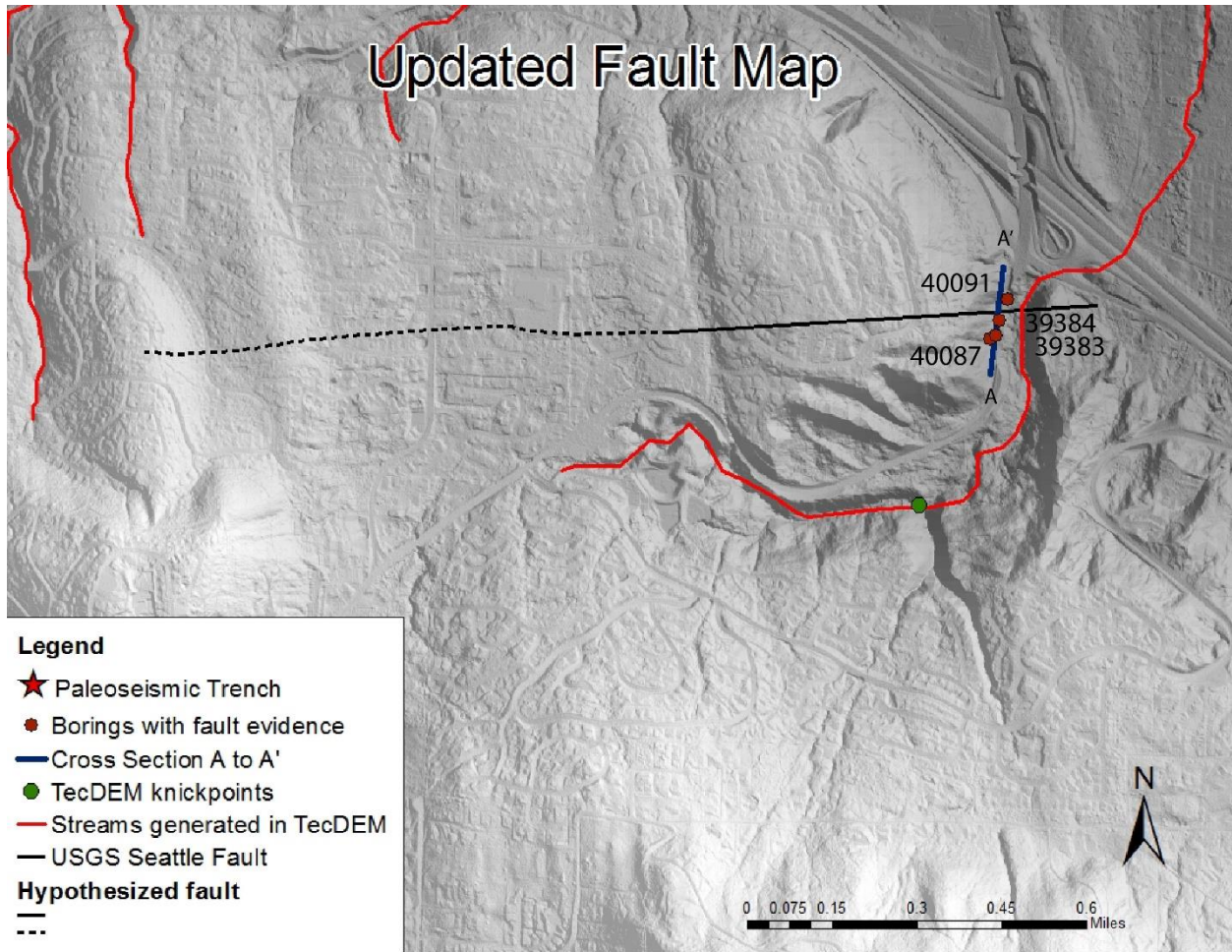


Figure 28. Boreholes containing evidence consistent with faulting. See Table 1 for boring logs containing fault evidence. Solid black line indicates the length along which boreholes contained fault indications, the dashed portion represents the boundary between shallower bedrock depths to the north and deeper bedrock depths to the south.

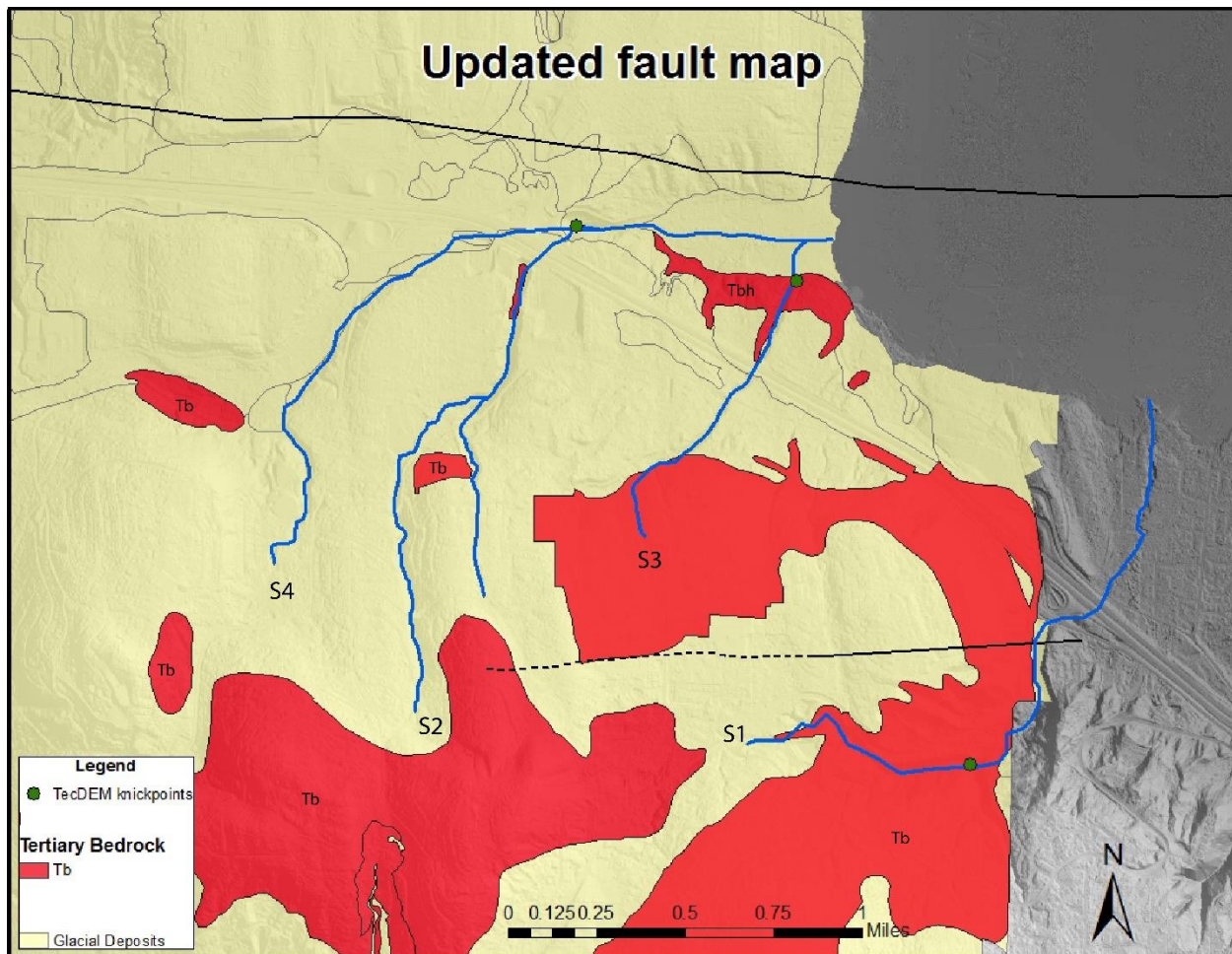


Figure 29. Simplified geologic map of Bellevue. Tertiary Blakeley Formation is labeled as Tb and the Tertiary Blakeley Harbor Formation is labeled as Tbh. Streams analyzed in TecDEM are indicated in blue. The hypothesized fault offset is indicated with the solid black line. The dashed portion is inferred based on shallower bedrock depths to the north and deeper bedrock depths to the south.

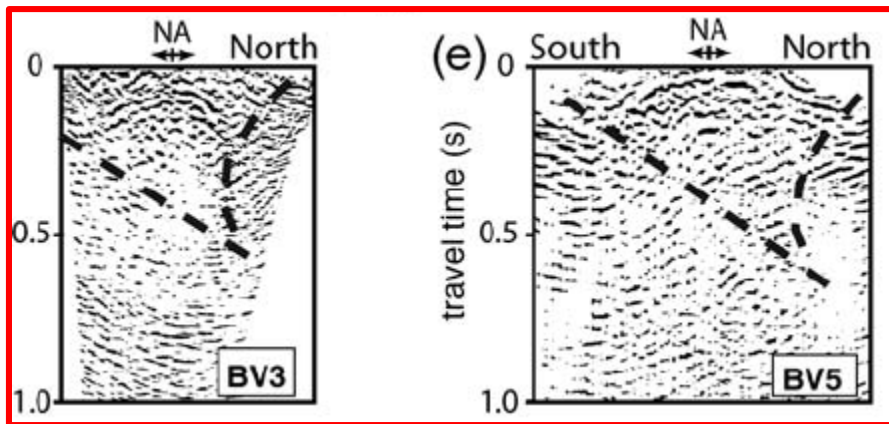
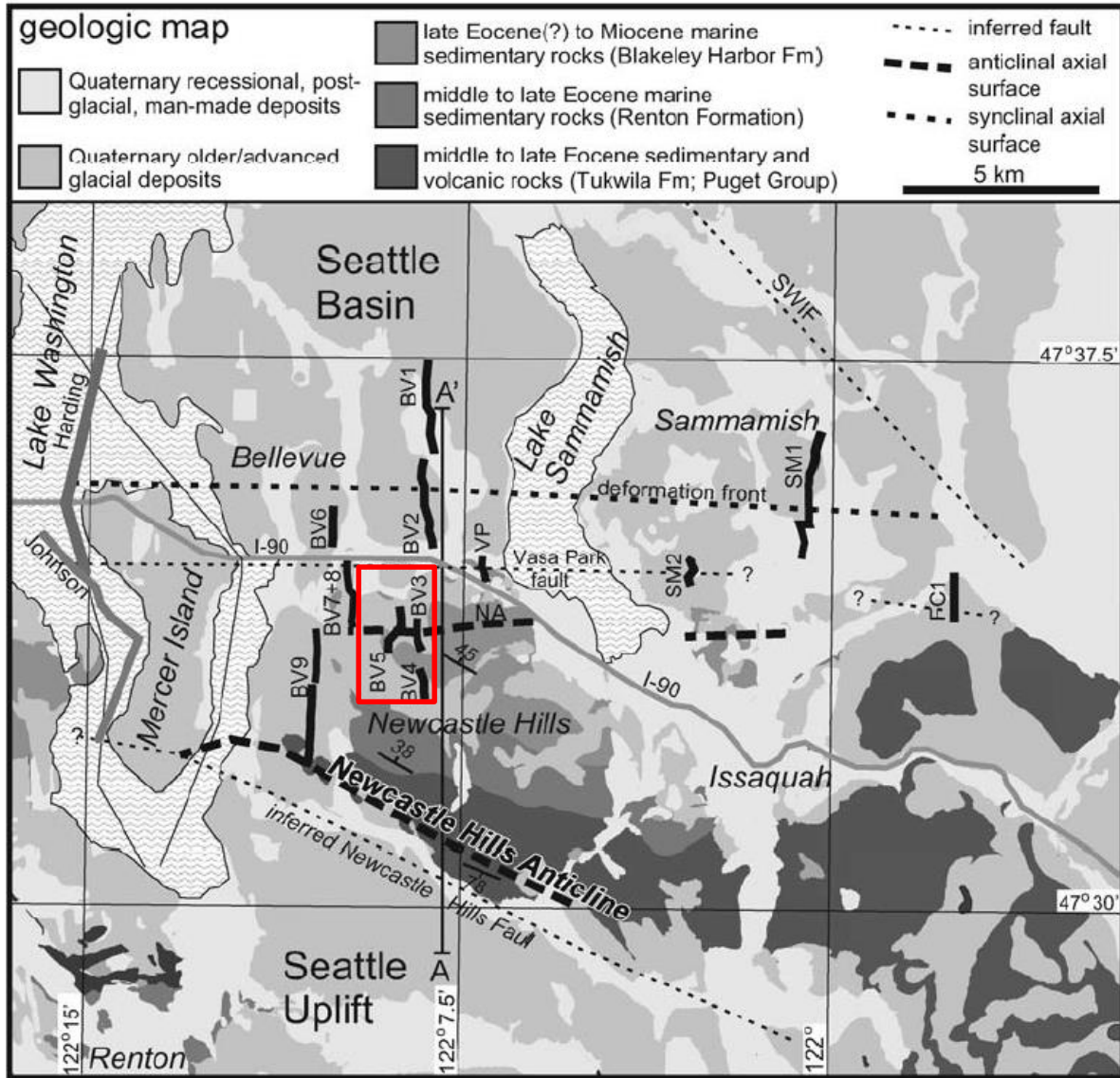


Figure 30. Seismic data, Liberty and Pratt, 2008. Seismic lines BV3 and BV5 illustrate the same backthrust identified in the borehole data.

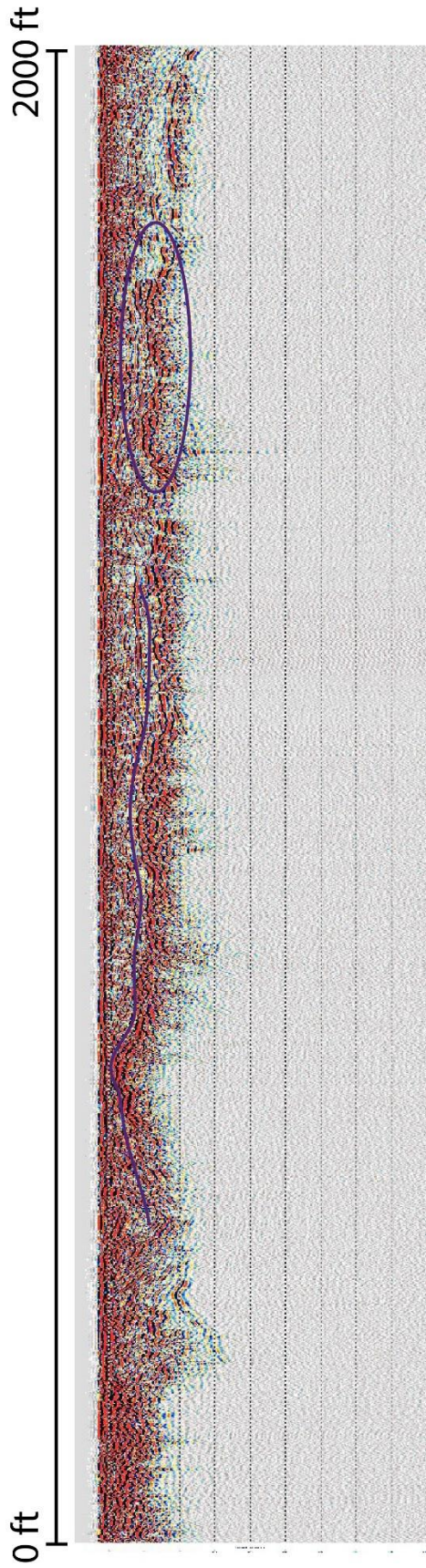


Figure 31. GPR Data. Survey line from Sunset Ravine (circled in yellow on Figure 31). This survey shows a reflective surface (purple line) that is likely part of the glacial stratigraphy and not associated with faulting. This could represent a compaction surface from a previous glacial cycle. Purple circle indicates reflective surfaces that resemble either push moraines or glacial till (van Overmeeren, 1998).

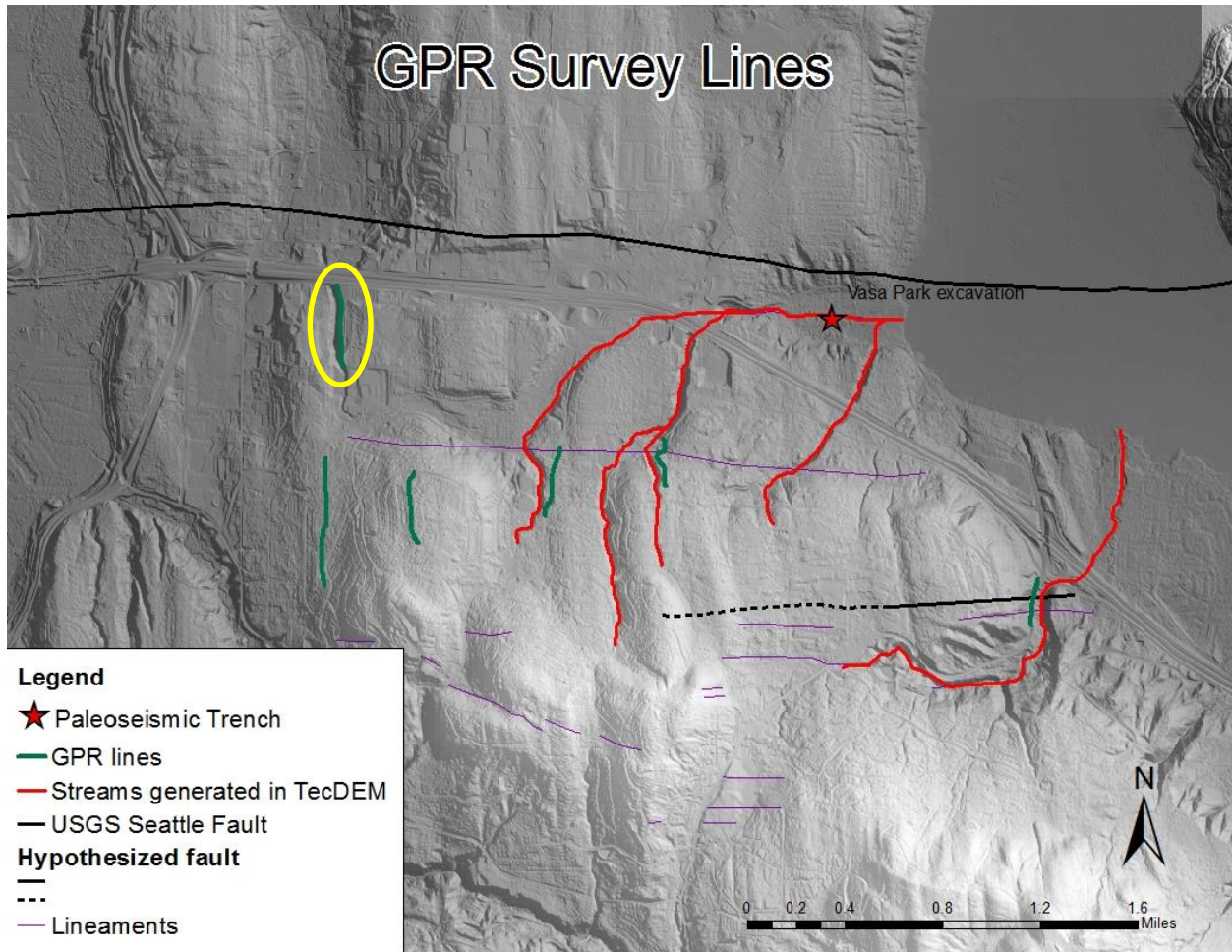


Figure 32. GPR Survey Lines. Green lines indicate the location of GPR survey lines throughout Bellevue. Yellow circle indicates the location of the GPR line shown in Figure 31. Ground and subsurface conditions prohibited radar penetration and data clarity.

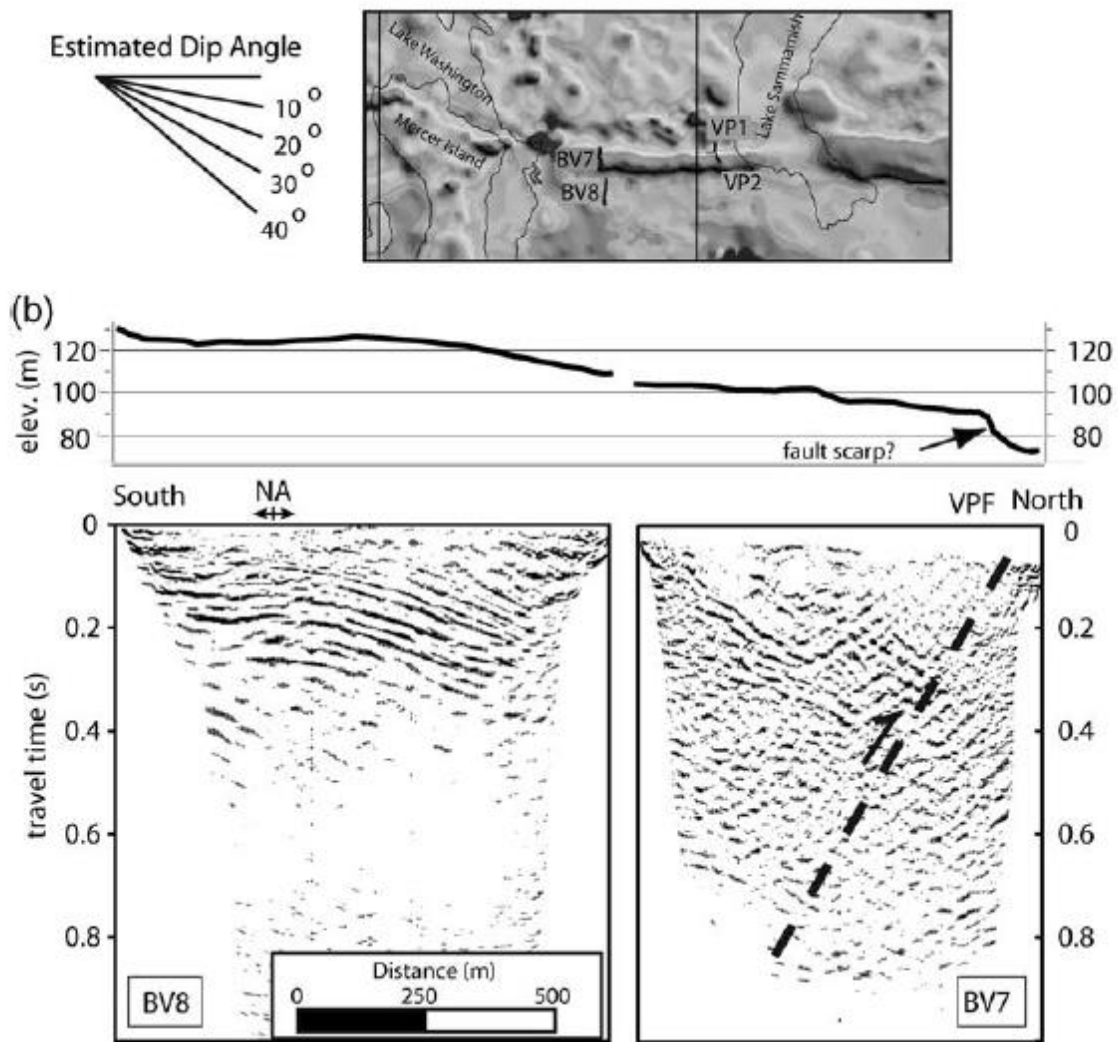


Figure 33. Liberty and Pratt (2008) seismic data illustrating an interpreted south-dipping thrust fault at the location where streams deflect. Refer to Figure 30 for fault location. The topographic profile labeled (b) illustrates the possible fault scarp location. Gravity map at the top of the figure shows the location of seismic lines BV8 and BV7. Liberty and Pratt's hypothesized fault scarp is not identifiable in my geomorphic analysis of streams that cross it. However, this topographic feature (and potential fault strand) does affect the plan view shape of the streams.